AD-A038 067 DREXEL UNIV PHILADELPHIA PA DEPT OF MECHANICAL ENGIN--ETC F/G 21/5
DYNAMIC BEHAVIOR OF LAMINATED POLYMERIC MATRIX COMPOSITES.(U)
JUL 76 R W MORTIMER, P C CHOU F33615-73-C-5102

UNCLASSIFIED AFML-TR-76-127 NL

1 OF 1
ADA038067

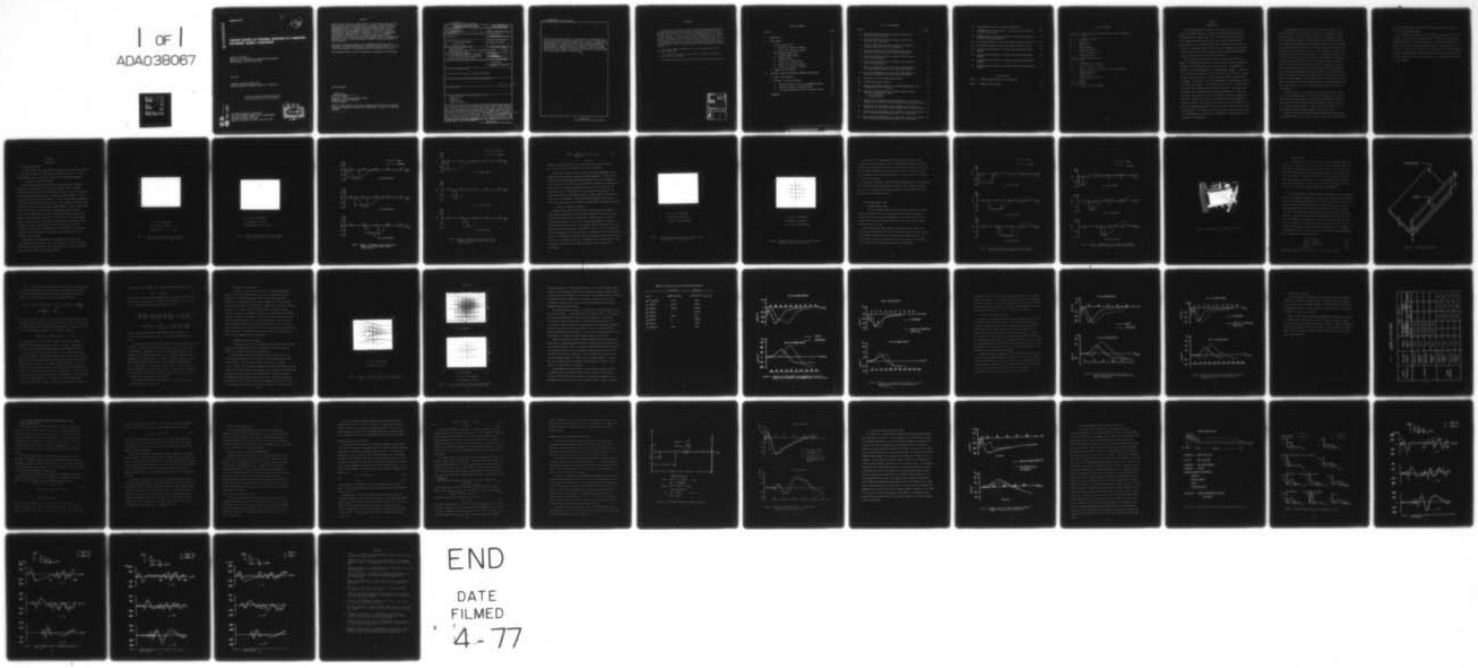

END

DATE
FILMED
4-77

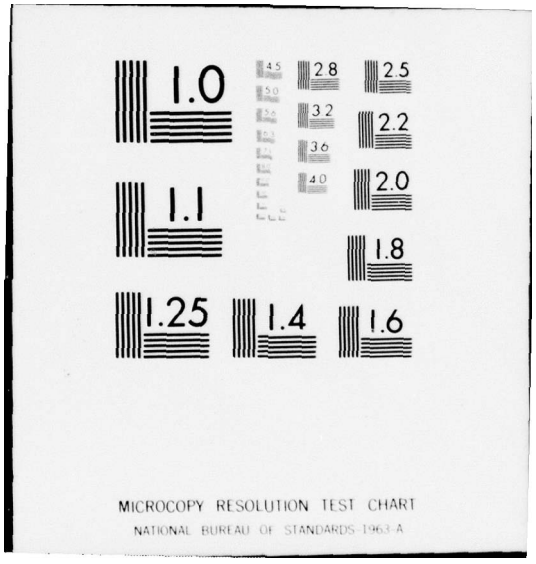
1.0
1.1
1.25
1.4
1.6
1.8
2.0
2.2
2.5
2.8
3.2
3.6
4.0
4.5
5.0
MICROCOPY RESOLUTION TEST CHART
NATIONAL BUREAU OF STANDARDS-1963-A

AFML-TR-76-127

(12)

FURTHER STUDIES OF DYNAMIC BEHAVIOR OF LAMINATED POLYMERIC MATRIX COMPOSITES

DREXEL UNIVERSITY
MECHANICAL ENGINEERING & MECHANICS DEPARTMENT
PHILADELPHIA, PENNSYLVANIA 19104

JULY 1976

TECHNICAL REPORT AFML-TR-76-127
ANNUAL REPORT FOR PERIOD MARCH 1974 - MARCH 1975

AIR FORCE MATERIALS LABORATORY
AIR FORCE WRIGHT AERONAUTICAL LABORATORIES
AIR FORCE SYSTEMS COMMAND
WRIGHT-PATTERSON AIR FORCE BASE, OHIO 45433

NOTICE

When Government drawings, specifications, or other data are used for any purpose other than in connection with a definitely related Government procurement operation, the United States Government thereby incurs no responsibility nor any obligation whatsoever; and the fact that the Government may have formulated, furnished, or in any way supplied the said drawings, specifications, or other data, is not to be regarded by implication or otherwise as in any manner licensing the holder or any other person or corporation, or conveying any rights or permission to manufacture, use, or sell any patented invention that may be related in any way thereto.

This report has been reviewed by the Information Office (IO) and is releasable to the National Technical Information Service (NTIS). At NTIS, it will be available to the general public, including foreign nations.

This technical report has been reviewed and is approved for publication.

FOR THE DIRECTOR

S. W. TSAI, Chief
Mechanics & Surface Interactions Branch
Nonmetallic Materials Division
Project Engineer

Copies of this report should not be returned unless return is required by security considerations, contractual obligations, or notice on a specific document.

AIR FORCE - 30 MARCH 77 - 200

UNCLASSIFIED

SECURITY CLASSIFICATION OF THIS PAGE (When Data Entered)

REPORT DOCUMENTATION PAGE

READ INSTRUCTIONS BEFORE COMPLETING FORM

1. REPORT NUMBER: AFML-TR-76-127	2. GOVT ACCESSION NO.
3. RECIPIENT'S CATALOG NUMBER	
4. TITLE (and Subtitle): Dynamic Behavior of Laminated Polymeric Matrix Composites	5. TYPE OF REPORT & PERIOD COVERED: Annual 15 Mar 74 - 15 Mar 75
	6. PERFORMING ORG. REPORT NUMBER
7. AUTHOR(s): Dr. Richard W. Mortimer; Dr. Pei C. Chou	8. CONTRACT OR GRANT NUMBER(s): F33615-73-C-5102
9. PERFORMING ORGANIZATION NAME AND ADDRESS: Drexel University, Mechanical Engineering & Mechanics Department, Philadelphia, Pa. 19104	10. PROGRAM ELEMENT, PROJECT, TASK AREA & WORK UNIT NUMBERS: 73420201 02
11. CONTROLLING OFFICE NAME AND ADDRESS: Air Force Materials Laboratory (AFML/MBM), Air Force Wright Aeronautical Laboratories, Wright-Patterson AFB, OHIO 45433	12. REPORT DATE: July 1976
	13. NUMBER OF PAGES: 58
14. MONITORING AGENCY NAME & ADDRESS (if different from Controlling Office)	15. SECURITY CLASS. (of this report): UNCLASSIFIED
	15a. DECLASSIFICATION/DOWNGRADING SCHEDULE

16. DISTRIBUTION STATEMENT (of this Report)

Approved for Public Release; distribution unlimited

17. DISTRIBUTION STATEMENT (of the abstract entered in Block 20, if different from Report)

390 782

18. SUPPLEMENTARY NOTES

19. KEY WORDS (Continue on reverse side if necessary and identify by block number)

Dynamic Behavior
Composites
Laminated Plates
Impact of Composites

20. ABSTRACT (Continue on reverse side if necessary and identify by block number)

The purpose of this document is to present the results of the second year's (March 15, 1974 to March 15, 1975) work on AFML Contract No.F33615-73-C-5102. The primary goal of this two-year program is to study, numerically and experimentally, the dynamic response of idealized laminated graphite-epoxy fan blades subjected to impact loads. The blade is simulated by a flat plate. Two impact cases are studied: one is the inplane impact, the other is the shear-bending impact. For each case, both numerical calculation and experimental tests are conducted. The calculations are based on a lamination theory and a method of characteristics code. The experiments involve pendulum plate impact and air gun accelerated projectile impact.

DD FORM 1 JAN 73 1473 EDITION OF 1 NOV 65 IS OBSOLETE

UNCLASSIFIED

SECURITY CLASSIFICATION OF THIS PAGE (When Data Entered)

20. This report includes results of the theoretical and experimental predictions of wave velocities and strain histories for the cases of in-plane and shear-bending impact of aluminum, graphite-epoxy cross-ply, and graphite epoxy angle-ply plates. In addition, the status of the program to compute local responses (using the finite-difference code HEMP) and structural responses (using NASTRAN) of laminated structures is presented. Finally, preliminary results of an impact parametric study (utilizing NASTRAN) involving the impact of a laminated beam structure are presented.

FOREWORD

This report was prepared by Drexel University, Mechanical Engineering and Mechanics Department, Philadelphia, Pennsylvania, 19104 under Air Force Contract F33615-73-C-5102. The principal investigators are Dr. Richard W. Mortimer and Dr. Pei C. Chou. The Air Force Project Monitor is Dr. Stephen W. Tsai, AFML/MBM of the Mechanics and Surface Interactions Branch, Non-metallic Materials Division, Air Force Materials Laboratory, Wright-Patterson Air Force Base, Ohio 45433. Research was conducted under Project 7342, "Fundamental Research in Macromolecular Materials and Lubrication Phenomena," Task No. 734002, "Studies on the Structure-Property Relationship of Polymeric Materials."

This report covers work performed during the period 15 March 1974 through 15 March 1975.

The report was released by the authors, Dr. Richard W. Mortimer and Dr. Pei C. Chou, in June 1975.

This technical report has been reviewed and is approved for publication.

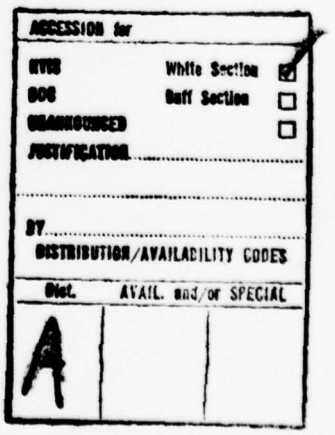

TABLE OF CONTENTS

LIST OF ILLUSTRATIONS

LIST OF TABLES

LIST OF SYMBOLS

A_{ij}, D_{ij}, I, P - plate coefficients and plate mass terms as defined in Ref. 2.

b = thickness of striker

c_0 = $(A_{11}/P)^{1/2}$

c_3 = $(kA_{55}/P)^{1/2}$

E = Young's Modulus

h = specimen thickness

k = shear correction factor

ℓ = length of striker

M_x, M_{xy}, Q_x = moments and shear force

t = time

u = z-displacement for striker

V_0 = initial velocity of striker

x = spatial coordinate in direction of wave propagation

w = specimen deflection

ν = Poisson's ratio

σ = normal stress in striker

ρ = density

ψ_x, ψ_y = rotations

ε = normal strain for specimen

SECTION I

INTRODUCTION

This report presents the results for the second year's work on the study of the dynamic response of idealized laminated graphite-epoxy fan blades subjected to impact loads. Due to the complexity of the geometry of the blade, detailed fiber-by-fiber, or ply-by-ply, "micro-mechanic" stress analysis is not feasible at this time; laminated plate theory must be used. The primary purpose of this study is to demonstrate the accuracy of the equations derived from lamination theory by comparing experimental results with those calculated from these equations.

Both in-plane and shear-bending impact results are included in the Report. The experimental phase of the present study consists of impacting the edge of the specimen plate with a striker plate. The experiment is designed to permit measurements of a one-dimensional response. The velocity of the impact is maintained at a low level such that the response is purely elastic. The pulse shape of the impact loading function is approximately rectangular. The duration of the resulting impact is controlled by varying the striker plate length. The strain histories are used for comparison with the analytically predicted wave velocities and strains. Additional gages are mounted on the plate specimens to monitor simultaneity of impact and uniformity of strains across the plate thickness as the wave propagates into the plate. Three specimen plates are tested and the results compared to analytical results. One specimen plate is fabricated from aluminum, and the other two from graphite-epoxy, one is layed-up as a cross-ply and the other as an angle-ply. The aluminum plate has been used to ascertain the accuracy of the experimental set-up since wave propagation in aluminum structures is reasonably well understood.

The laminated plate equations used in this report are those derived by Whitney and Pagano [2]. As discussed in [3], this set of equations is more accurate than that of [4], and may be considered as a representative "first order" laminated plate theory. Several analytical and numerical solutions to the laminated plate equations have been presented recently. Wang and Tuckmantel [5], and Moon [6] have discussed the wave surfaces based on the laminated plate equations due to abrupt change in stress. Chow [7] applied the Laplace transform technique and calculated the deflection of a laminated plate under a concentrated load. Moon [8] solved the problem of one-dimensional wave propagation due to a prescribed line load by the fast Fourier transform technique. Recently, Sun and Lai [9] analyzed the response of a unidirectional fiber-reinforced layer subjected to lateral loading by applying transform techniques to the laminated plate equations and exact equations. Several experimental studies on the dynamic response of composites have been reported in Ref. [10-13]. However, the major emphasis of these studies has been to determine the elastic moduli and dispersive nature of composite materials; no work involving the transient strain histories of realistic laminated plates subjected to impact has been presented.

Detailed description of the general set-up of this program can be found in the first annual report, Ref. 14 and will not be repeated here. This includes the governing equations used, the numerical procedures, the specimen preparation, the in-plane impact experiment arrangement, and the results of the in-plate aluminum plate impact. Many of the results reported here have also appeared in previous quarterly progress reports, Ref. [15-17].

Results of this study demonstrate that the laminated plate theory used here adequately predicts the wave velocities and transient strains in symmetric

cross-ply and angle-ply composite plates under either in-plane impact or transverse shear-bending impact.

Also included in this Report is a discussion of our progress in the use of HEMP, a finite-difference computer code, to predict material responses, and NASTRAN to predict structural responses. In addition, we present preliminary results of an impact parametric study utilizing NASTRAN for the calculations. The goal of this study is to identify which of the loading function parameters (pulse duration, pulse shape, object kinetic energy, and impulse) are most important for the structural response of a laminated beam subjected to impact loading.

SECTION II

PLATE IMPACT

1. IN-PLANE IMPACT STUDY

The description of the experimental set-up and the theoretical calculation of the in-plane impacts have been reported previously in Ref. 14. Here we shall present directly new results obtained for the composite specimens.

a. Results for Cross-Ply Laminate

Typical results from the strain histories monitored on the graphite-epoxy cross-ply laminated plate are shown in Figures 1 and 2. Figure 1 includes the results for the 76.2 mm striker and Figure 2 the 25.4 mm striker. The strain gage numbers are shown to the right of the photographs. Observation of the strain histories from gages 2, 4, and 5 show that good simultaneity of impact has been achieved for both strikers. The maximum difference between wave arrival times at the three gages was approximately 6 μsec; the magnitudes of the strain pulse at each of these three gages were nearly identical. Gages 2 and 2R demonstrate that little bending was induced by either of the impacts. The average wave velocities (7.71 mm/μsec for the 76.2 mm striker and 7.70 mm/μsec for the 25.4 mm striker) measured from the pulse initiation at gages 1, 2, and 3 agrees with the theoretical velocity, $(A_{11}/P)^{\frac{1}{2}}$ = 7.55 mm/μsec, with A_{11} = 0.713 MN/mm and P = 0.0125 gm/mm^2 for the laminated specimen. These three gages also show that the initial pulse has little attenuation or dispersion.

Comparisons of the experimental and analytically predicted strain histories are shown in Figures 3 and 4. The analytical results are based on the solution of equation (4a) of Ref. 14 subjected to zero initial conditions and a boundary condition at the impacted edge of

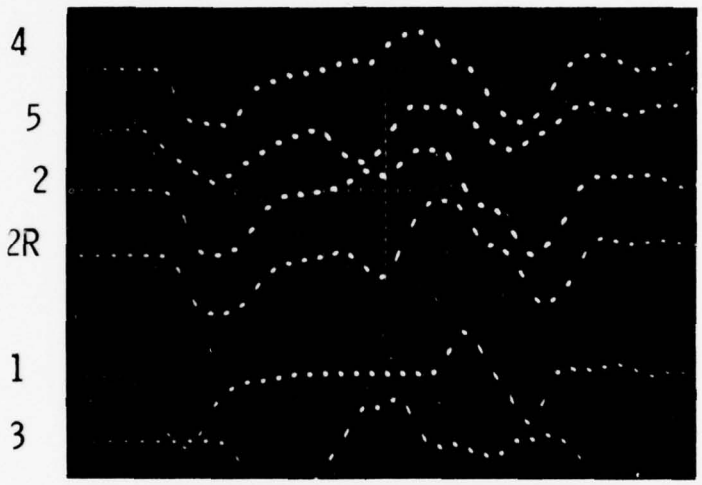

20 μsec/div. HORIZONTAL

187 μmm/mm/div. VERTICAL

STRIKER VELOCITY = 2.423 m/sec.

Figure 1. Typical Oscilloscope Traces for Graphite Epoxy Cross-Ply Plate (76.2 mm Striker).

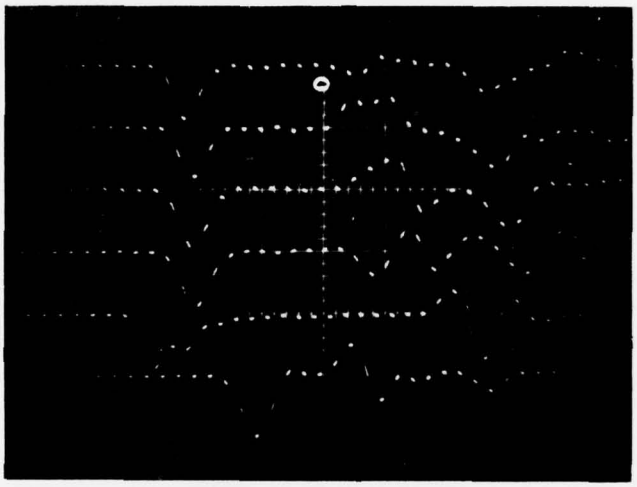

20 μsec/div. HORIZONTAL

187 μmm/mm/div. VERTICAL

STRIKER VELOCITY = 2.617 m/sec.

Figure 2. Typical Oscilloscope Traces for Graphite Epoxy Cross-Ply Plate (25.4 mm Striker).

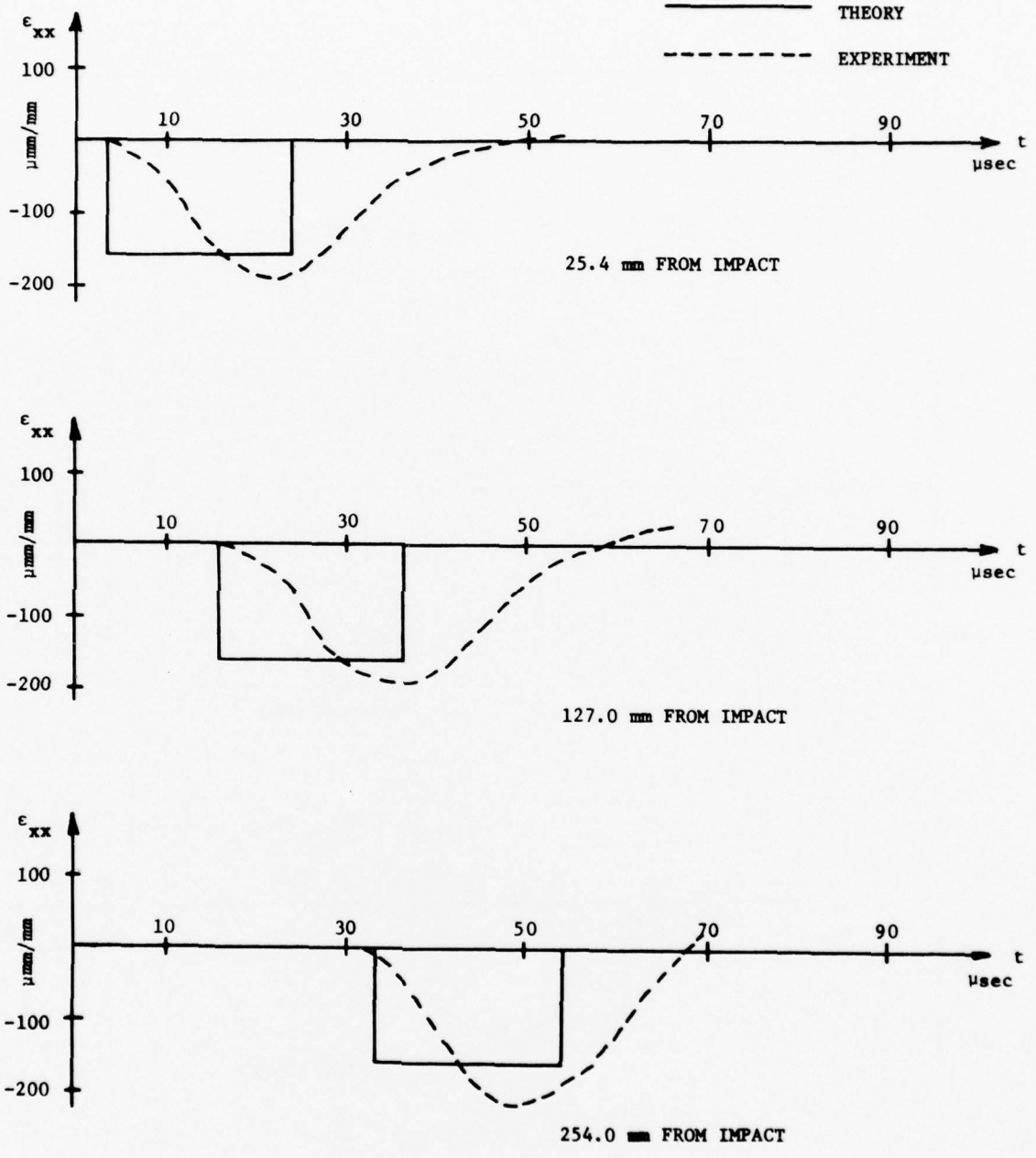

Figure 3. Theory vs. Experiment for the In-Plane Strain Response of the Graphite-Epoxy Cross-Ply (76.2 mm Striker).

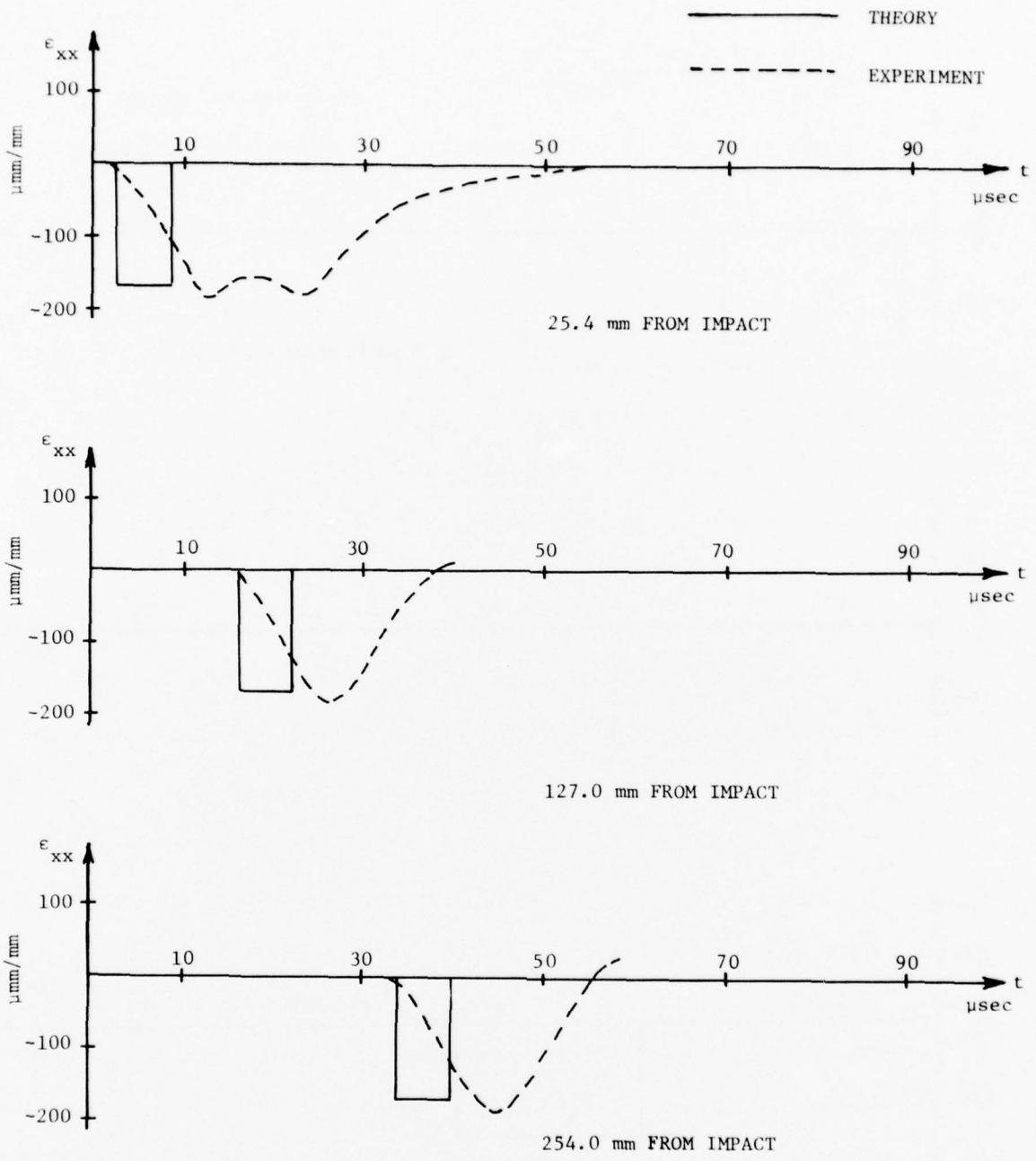

Figure 4. Theory vs. Experiment for the In-Plane Strain Response of the Graphite-Epoxy Cross-Ply Plate (25.4 mm Striker).

$$\varepsilon_0(0,t) = \frac{V_0}{2(A_{11}/P)^{\frac{1}{2}}} \quad \text{for } 0 \leq t \leq t_0 \qquad (1)$$

$$= 0 \qquad \text{for } t_0 < t$$

where t_0 = 20.19 μsec and V_0 = 2.423 m/sec for the 76.2 mm striker and t_0 = 6.73 μsec and V_0 = 2.617 m/sec for the 25.4 mm striker.

Observation of Figures 3 and 4 show that the strain magnitudes of the experimental and analytical results are in good agreement. For the 76.2 mm striker the average experimental pulse duration was 35 μsec as compared to the theoretical value of 20.19 μsec; for the 25.4 mm striker the experimental value was 18 μsec versus a theoretical value of 6.73 μsec. Much of this difference is due to the delay in the strain gage circuit response. The experimental shape is approximately that of a $\sin^2$, whereas, the theoretical pulse shape is rectangular. This discrepancy in shape is to be expected since the strain gages can not measure discontinuities in loading or unloading.

b. Results for Angle-Ply Laminate

Typical results from the strain histories monitored on the graphite-epoxy angle-ply laminated plate are shown in Figures 5 and 6 for the 76.2 mm striker and 25.4 mm striker, respectively. Observation of these strain histories from gages 2, 4, and 5 show that good simultaneity of impact has been achieved for both strikers. Also, gages 2 and 2R demonstrate that little bending was induced by either of the impacts. Gages 1, 2, and 3 demonstrate that the average measured wave velocities, 7.54 mm/μsec for the 76.2 mm striker and 7.32 x 10^6 mm/μsec for the 25.4 mm striker, agree well with the theoretical velocity of 7.39 mm/μsec where A_{11} = 0.584 MN/mm and P = 0.0107 gm/mm^2. These three gages also show that the initial pulse has little attenuation or dispersion.

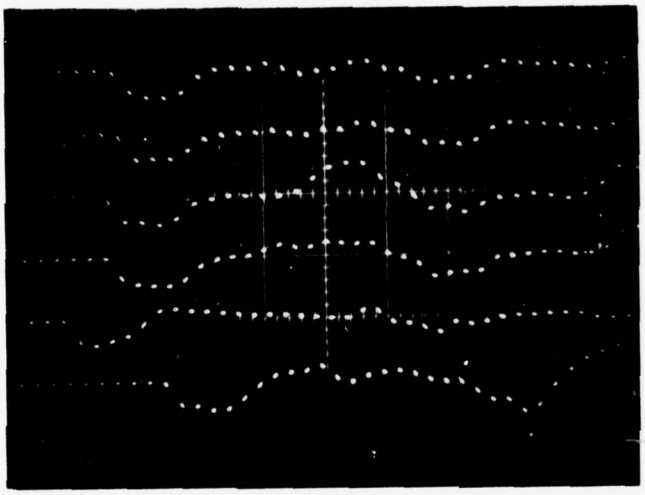

20 μsec/div. HORIZONTAL

400 μmm/mm/div. VERTICAL

2.55 m/sec. STRIKER VELOCITY

Figure 5. Typical Oscilloscope Traces for Graphite Epoxy Angle-Ply Plate (76.2 mm Striker).

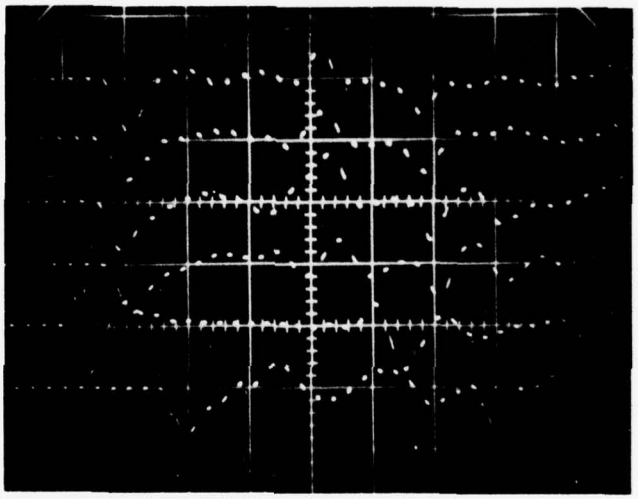

20 μsec/div. HORIZONTAL

200 μmm/mm/div. VERTICAL

2.55 m/sec. STRIKER VELOCITY

Figure 6. Typical Oscilloscope Traces for Graphite Epoxy Angle-Ply Plate (25.4 mm Striker)

Comparisons of the experimental and analytically predicted strain histories are shown in Figures 7 and 8. The analytical results are based on the solution of equation (3a) of Ref. 14 subjected to zero initial conditions and the boundary condition given in equation (1), with t = 20.62 μsec and V = 2.55 m/sec for the 76.2 mm striker and t_0 = 6.87 μsec and V = 2.55 m/sec for the 25.4 mm striker.

Observation of Figures 7 and 8 show that the magnitude of the experimental and analytical strain pulse agree well, while the pulse duration and shape do not. The discussion of the possible reasons for these discrepancies has been given in the previous Section.

2. Shear-Bending Impact Study

a. Pendulum Impact System

The basic pendulum impact system previously designed for in-plane impacts is utilized for the shear-bending impact system (see Figure 9). The only difference is that the specimen plate is oriented such that the striker plate strikes the specimen along its top surface (near the edge) rather than along its edge.

The specimen plate, gage locations, velocity measuring system, and strain gages are identical to the in-plane impact system. The only difference is that gages 2 and 2R are used to ensure a uniform bending impact. The strain traces from these two gages should be exactly opposite in magnitude (e.g. top surface in tension, bottom surface in compression).

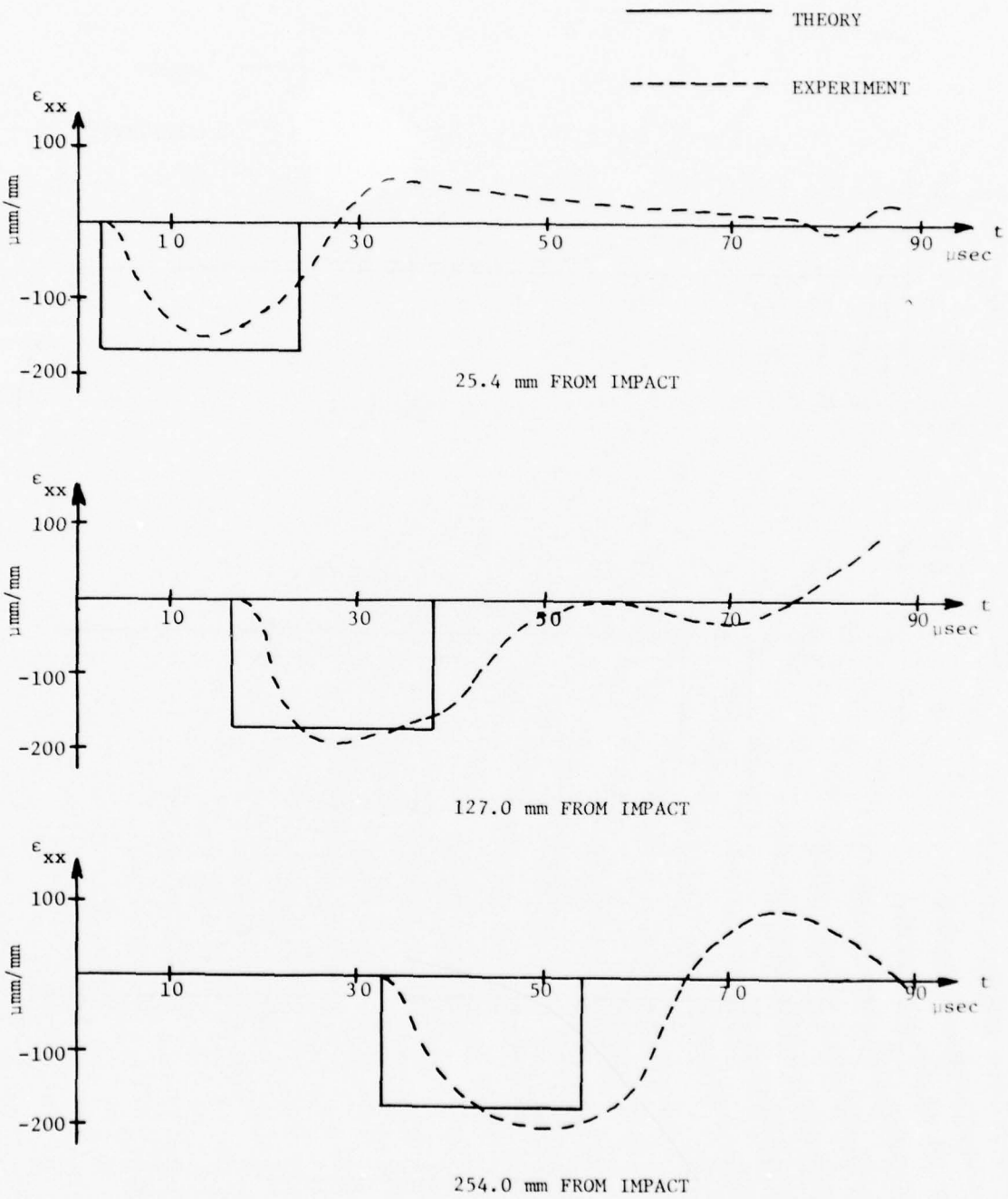

Figure 7. Theory vs. Experiment for the In-Plane Strain Response of the Graphite Epoxy Angle-Ply Plate (76.2 mm Striker).

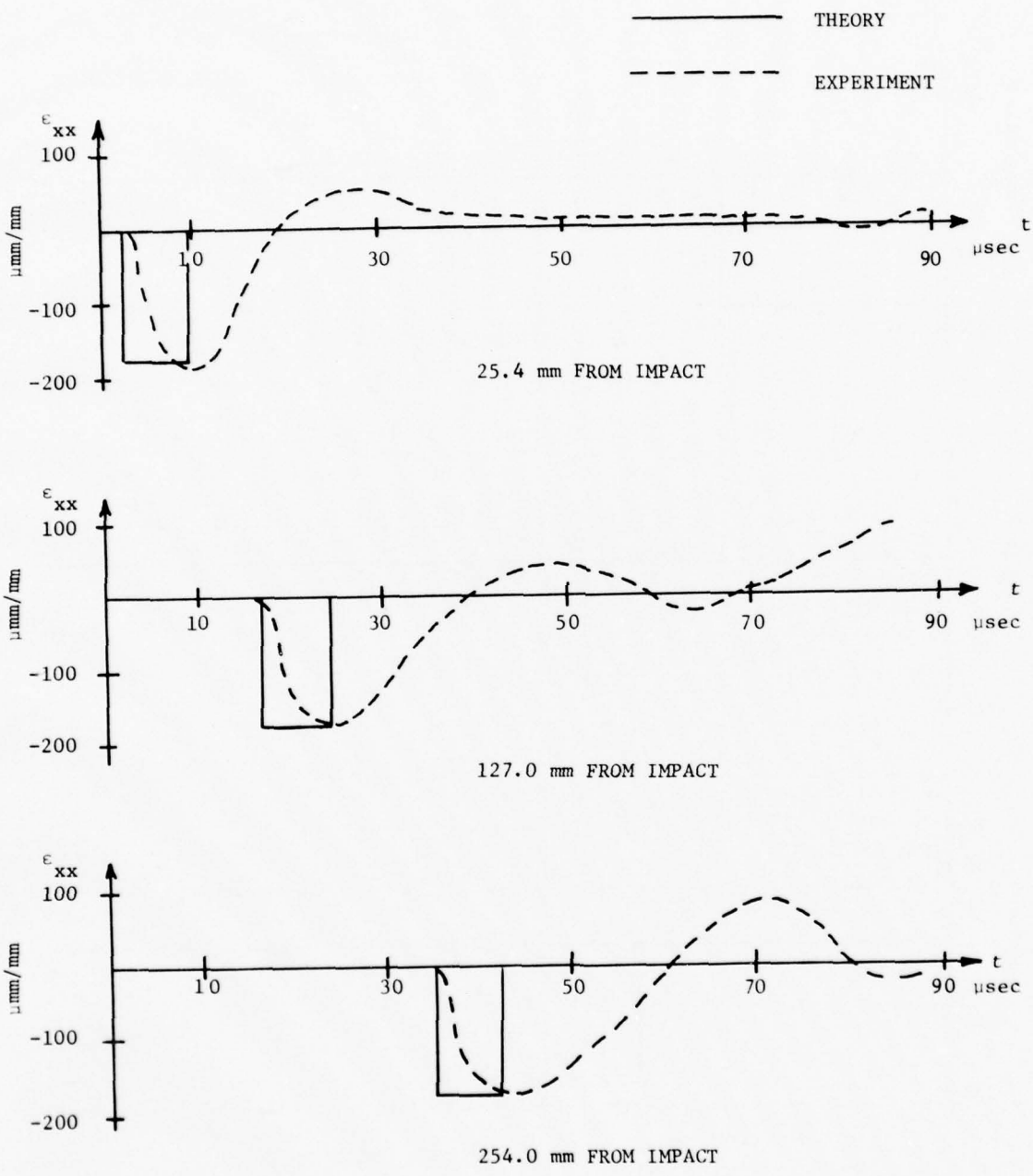

Figure 8. Theory vs. Experiment for the In-Plane Strain-Response of the Graphite Epoxy Angle-Ply Plate (25.4 mm Striker).

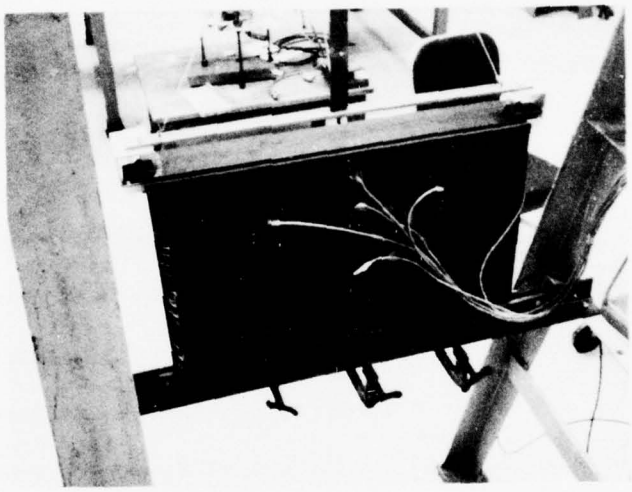

Figure 9. Photograph of Shear-Bending Impact System

b. Loading Function

The loading function for the specimen in the transverse impact case depends on the wave motion in the striker and cannot be specified explicitly beforehand. Instead, the wave motions in the striker and the specimen are solved simultaneously, with certain matching conditions at the contact interface. The striker is assumed to have pure in-plane motion, governed by the simple wave equation. The motion of the entire specimen plate is assumed to be in the shear-bending mode where the three-dimensional compression waves in the region close to the impact surface have been neglected.

The three second order differential equations governing the shear-bending motions of an angle-ply laminate, Eqs. (3c) of Ref. 14 require three boundary conditions at the impacted edge, x=0. The simple wave equation of the striker needs one boundary condition at z=0, where the wave motion in the plate is along x-direction and in the striker along negative z-direction, as shown in Fig. 10 . The four required boundary conditions are supplied at the impact surface x=0, z=0, by (a) matching the displacements of the striker and the plate, (b) equating the total axial force in the striker to the total shear force in the plate, (c) assuming the moment for the plate is equal to the force in the striker multiplied by half the striker thickness, and (d) assuming the moment M_{xy} is zero. If $\sigma(z,t)$ and $u(z,t)$ are the stress and displacement in the striker, then, these conditions are,

$$u(0,t) = w(0,t) \tag{2}$$

$$\sigma(0,t) = Q_x(0,t)/b \tag{3}$$

$$M_x(0,t) = \sigma(0,t)\ b^2/2 \tag{4}$$

$$M_{xy}(0,t) = 0 \tag{5}$$

where Q_x,M_x, and M_{xy} are the shear force and moments in the plate.

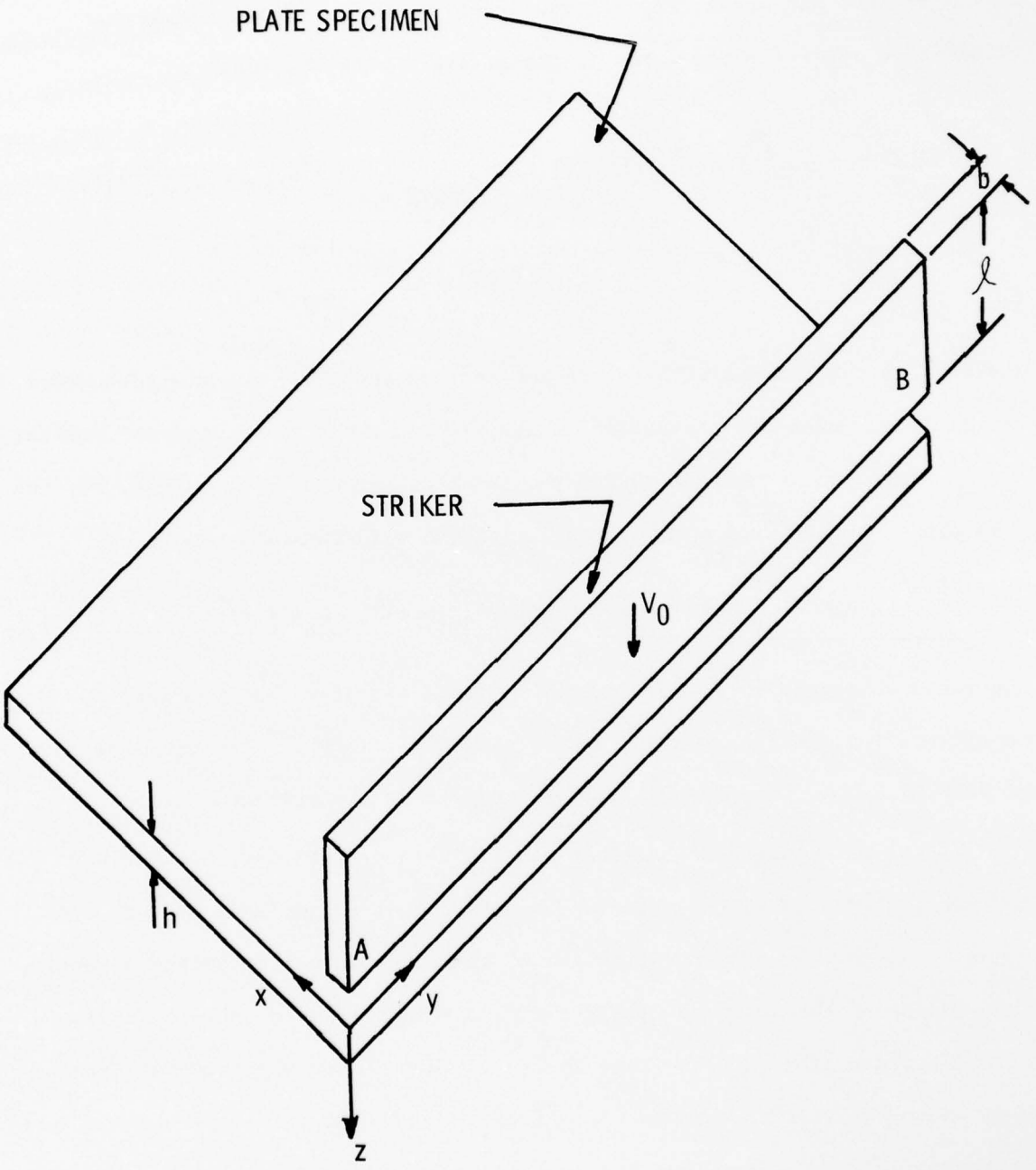

Figure 10. Shear-Bending Impact Geometry

For $t > 0$, a general relation between $\sigma(0,t)$ and $u_{,t}(0,t)$ can be derived. This is done by integrating the simple wave equation along characteristics in the striker and accounting for the jumps in the variables across the transmitted and reflected waves in the striker, with the result

$$\sigma(0,t) = -\rho c_0 \left[(-1)^{N-1} V_0 - u_{,t}(0,t) - \sum_{n=1,2..}^{N-1} 2(-1)^n u_{,t}\left(0, t - \frac{2n\ell}{c_0}\right) \right] \quad (6)$$

$$\text{for } \frac{2\ell(N-1)}{c_0} < t < \frac{2\ell N}{c_0}$$

where V_0 is the initial velocity of the striker and (N-1) denotes the number of completed round trip traverses of the wave in the striker. If the striker and specimen are in contact during the first traverse of a wave, eqs. (2) and (3) can be substituted in equation (6) (with N=1) yielding

$$\frac{1}{b} Q_x(0,t) = -\rho c_0 [V_0 - w_{,t}(0,t)], \quad 0 < t < \frac{2\ell}{c_0} \quad (7)$$

The three equations (4), (5) and (6) form a set of proper boundary conditions for the specimen during the time $0 < t < \frac{2\ell}{c_0}$. Equations (3c) of Ref. 14 are no longer coupled explicitly with the striker equation.

If the stress at the interface becomes zero or positive, the striker and specimen separate, the matching condition must be replaced by free edge conditions, and the subsequent motion of the specimen can be solved directly, independent of the striker. The probable time for separation to occur is at $N2\ell/c_0$, the time when the wave in the striker due to the original impact returns to the striker-specimen interface. To determine if separation occurs at these instants, the normal stress must be found immediately after the wave is reflected and transmitted at the interface. This is accomplished by assuming that both bodies remain in contact and by considering equations (2),

(3), and (6) for $t = \frac{2N\ell^+}{c_0}$, and the jump relationship between Q_x and $w_{,t}$

$$[Q_x] = - \rho c_3 h [w_{,t}] \tag{8}$$

where the bracket denotes discontinuous values of variable enclosed. This is a system of 4 equations at $t = \frac{2N\ell^+}{c_0}$ in the 4 unknowns σ, $u_{,t}$, $w_{,t}$, and Q_x. The resulting expression for the normal stress is

$$\sigma\left(0, \frac{2N\ell^+}{c_0}\right) = \frac{c_3 h}{c_0 b + c_3 h}\left[\frac{c_0 b}{c_3 h}\ \sigma\left(0, \frac{2N\ell^-}{c_0}\right) + \rho c_0\ u_{,t}\left(0, \frac{2N\ell^-}{c_0}\right)\right. \tag{9}$$

$$\left. - \rho c_0 (-1)^{N-1} V_0 + 2\rho c_0 \sum_{n=1,2,..}^{N-1} (-1)^n\ u_{,t}\left(0, \frac{2N\ell^+}{c_0} - \frac{2n\ell}{c_0}\right)\right]$$

If the value of the right hand side of equation (9) is equal to or greater than zero, separation occurs. If not, the bodies remain in contact.

The procedure for calculating the responses of the specimen when separation does not occur after the first traverse of the wave in the striker is straightforward. Equations (3c) of Ref. 14 are solved for $\frac{2\ell}{c_0} < t < \frac{4\ell}{c_0}$ subject to the boundary conditions (4), (5), and equation (6) with N=2 and equations (2) and (3) inserted. If, after $t = \frac{4\ell}{c_0}$, the striker still does not separate, equations (3c) of Ref. 14 are solved in the time regime $\frac{4\ell}{c_0} < t < \frac{6\ell}{c_0}$ subject to the boundary condition (4), (5), and equation (6) with N=3 and equations (2) and (3) inserted. This procedure is repeated for every $\frac{2\ell}{c_0}$ in time until the striker is shown to separate by equation (9) or sufficient calculations have been achieved.

The procedure for the cross-ply laminate is similar to that just outlined for the angle-ply laminate.

c. Results for Aluminum Plate

In order to check out the accuracy of the shear-bending impact system, a 2024-T351 aluminum plate, rather than a laminate specimen, was tested first. Typical preliminary results from the strain histories monitored on the aluminum plate are shown in Figure 11. The gage numbers are shown to the right of the photograph. Observation of the strain histories from gages 2, 4, and 5 show that good simultaneity of impact has been achieved. Gages 2 and 2R demonstrate that we have achieved uniform bending across the thickness of the plate. The wave velocity, as measured from the pulse initiation of gages 1, 2, and 3 was 3.264 mm/μsec.; this agrees well with the theoretical shear velocity of 3.11 mm/μsec (k = 1.0). The strain traces in Figure 11 also show the arrival of the wave reflecting from the back edge of the plate. Based on these preliminary results, we have concluded that this experimental system is satisfactory.

d. Results for Cross-Ply Laminate

Application of eq. (9) to the impacts involving the 76.2 mm striker showed that it would separate after $2\ell/c_0$ while the 25.4 mm striker was shown not to separate (Section II-2b) until $6\ell/c_0$.

Figure 12a presents typical results from the strain histories on the cross-ply laminate produced by the transverse shear-bending impact of the 76.2 mm striker. The trace numbers again refer to the strain gage in Fig. 1 of Ref. 14. At least four impact tests with almost identical strain history traces were obtained for each impact case. Again the strain histories from gages 2, 4, and 5 show that good simultaneity of impact was achieved. The maximum difference between wave arrival times at these three gages was approximately 5 μsec; except for gage 4, the magnitudes of the strain pulse at these gages were found to be essentially identical. The reason for the

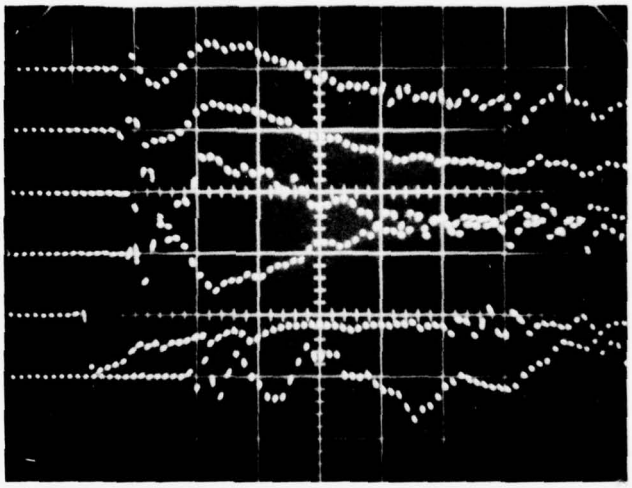

40 μsec/div. HORIZONTAL

400 μmm/mm/div. VERTICAL

Figure 11. Typical Oscilloscope Traces for the Shear-Bending Impact of an Aluminum Plate (76.2 mm Striker).

CROSS-PLY

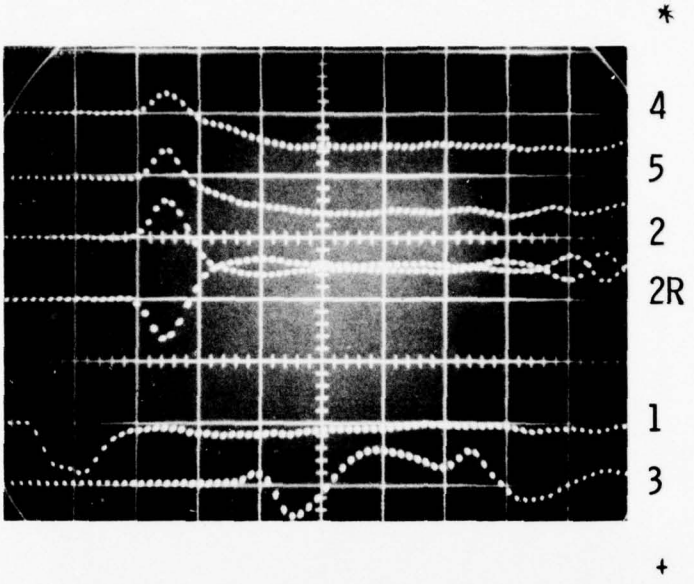

a. 76.2 mm STRIKER

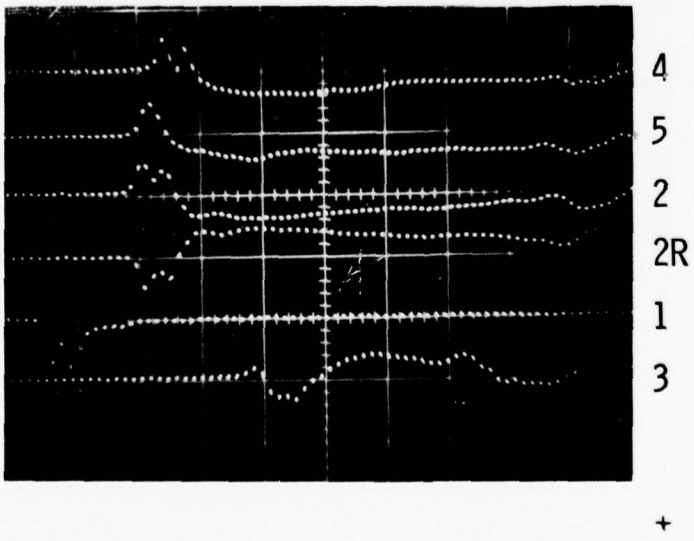

b. 25.4 mm STRIKER

40 μsec/div. HORIZONTAL

400 μmm/mm/div. VERTICAL

Figure 12. Typical Oscilloscope Traces for Graphite-Epoxy Cross-Ply Subjected to Shear-Bending Impact.

slight discrepancy in the magnitude at gage 4 is that, at the impact surface, uniform contact during the impact was not achieved, because of minute ripples on the surface of the laminate. For instance, for an impact speed of 2.5 m/sec, a 0.0254 mm (0.001") irregularity on the impact surface causes a 10 μsec discrepancy in arrival time. Gages 2 and 2R demonstrate that near perfect bending was induced by the impact.

The laminated plate properties are calculated from lamina properties and are listed in Table 1. The striker velocity V_0 was 2.55 m/sec. The average wave velocity determined from the peak strain at gages 1, 2, and 3 was 1.67 mm/μsec, which is much closer to the theoretical shear velocity of 1.53 mm/μsec, than the theoretical bending velocity of 7.69 mm/μsec, indicating that the pulse is primarily a shear wave. There is some uncertainty about the measured shear wave speed. For instance, if measured from the first disturbance at the gages, the shear velocity would be 1.81 mm/μsec.

Figure 13 shows that the pulse shape and magnitude of the experimental results are in general agreement with those from the theoretical calculation. The analytical strain at 25.4 mm contains a precursor bending wave travelling with the plate wave velocity, as indicated by the abrupt wave front. (The precursor at 127 mm is not plotted). The strain gage did not pick up this precursor, probably due to its limitation in frequency response. However, the fact that the bulk of the energy is travelling with a velocity nearly equal to the shear velocity is evident.

The experimental strain histories of the cross-ply laminate subjected to impact by the 25.4 mm striker were similar in nature to those of the 76.2 mm striker and are shown in Fig. 12b. The previous discussion of the experimental results also apply to this impact situation. Figure 14 presents

Table 1. Graphite/Epoxy Laminated Plate Properties

	Cross-ply	Angle-ply
Lay-up	$[(0_2^\circ/90^\circ)_8/0^\circ]_S$	$[(0^\circ/45^\circ/0^\circ/-45^\circ)_6, 0^\circ]_S$
$\rho(10^{-3}$ gm/mm$^3)$	1.511	1.511
A_{11} (MN/mm)	0.713	0.584
A_{55} (MN/mm)	0.0294	0.0269
A_{44} (MN/mm)	-	0.0267
D_{11} (MN-mm)	4.19	2.49
D_{16} (MN-mm)	0	-0.0491
D_{66} (MN-mm	-	0.506
c_0 (mm/μsec)	7.55	7.39

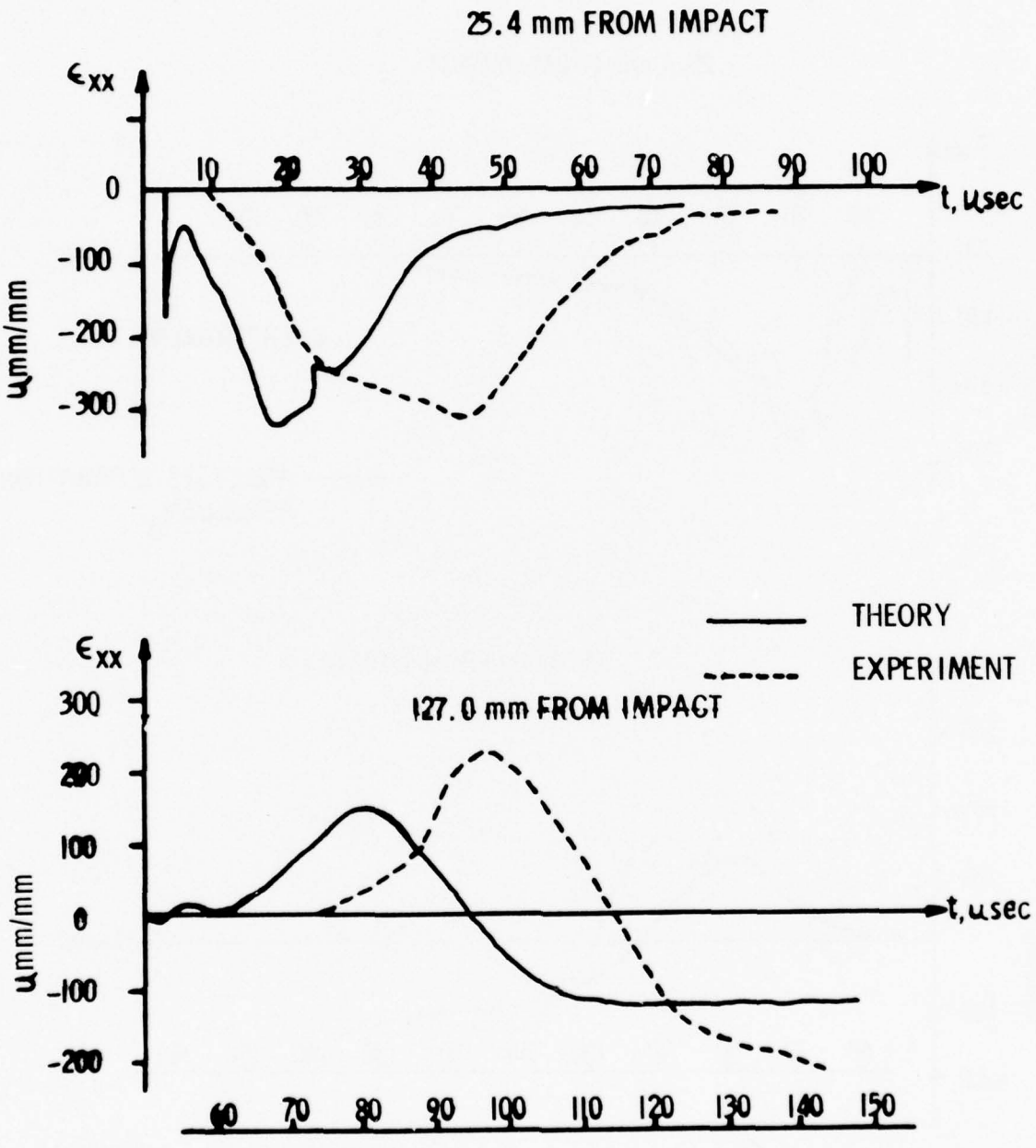

Figure 13. Theoretical and Experimental Strain Response of the Cross-Ply Laminate Due to Transverse (Shear-Bending) Impact (76.2 mm Striker)

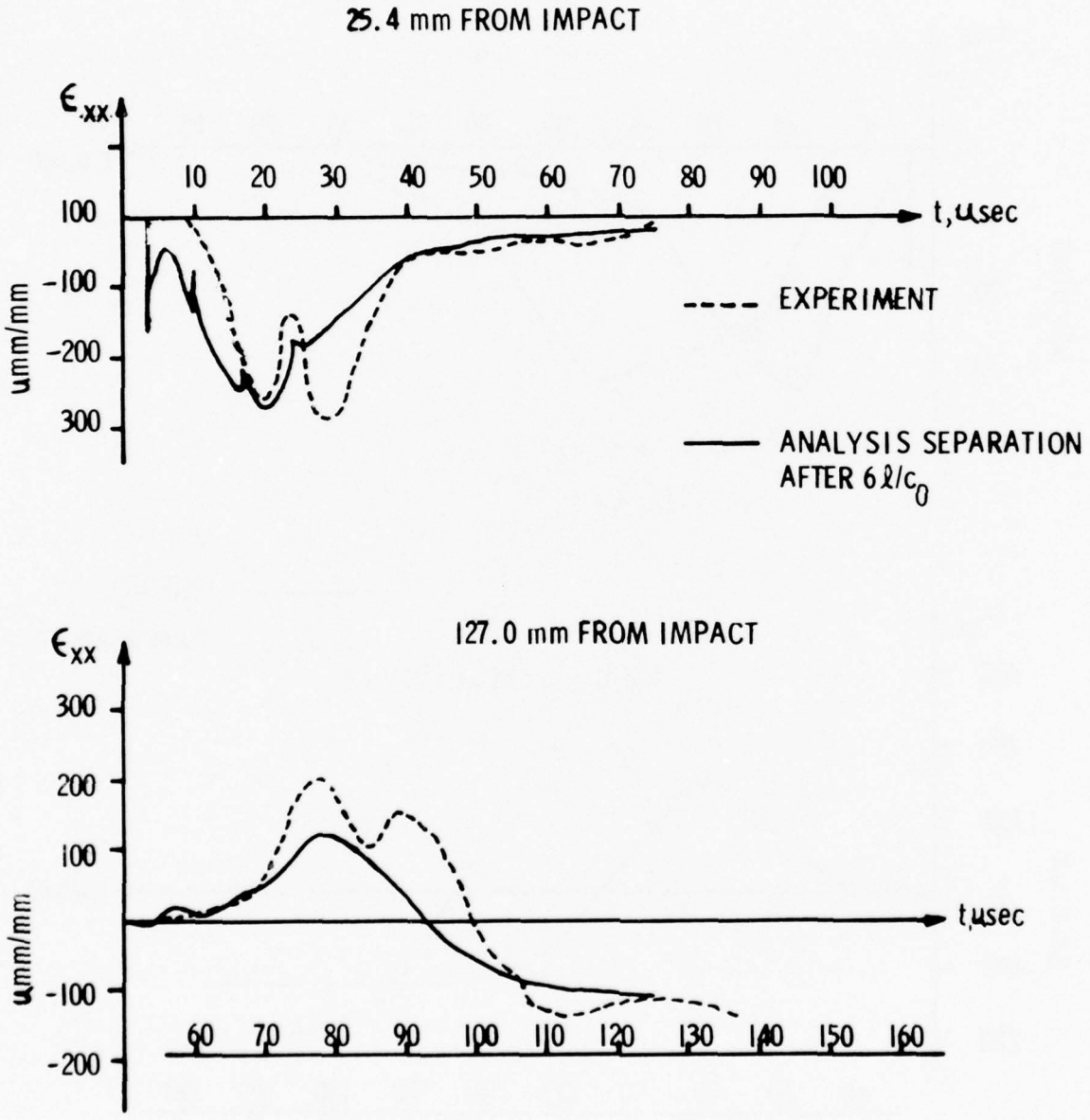

Figure 14. Theoretical and Experimental Strain Response of Cross-Ply Laminate Due to Transverse (Shear-Bending) Impact (25.4 mm Striker).

a comparison of the 25.4 mm striker induced strain histories on the cross-ply laminate with analysis. We note general agreement between the experimental and analytical pulse shapes and pulse magnitudes. The average velocity based on first disturbance was 1.90 mm/μsec and based on peak strain was 1.58 mm/μsec. The theoretical shear velocity for the cross-ply was 1.53 mm/μsec.

e. Results for Angle-Ply Laminate

Results of the angle-ply specimen subjected to transverse impact by the 76.2 mm striker are shown in Figure 15. The striker impact velocity V_0 is 2.55 m/sec. Application of eq. (9) to the impacts involving the 76.2 mm striker showed that it would separate after $2\ell/c_0$. The average of the measured wave velocities, based on first disturbance at gages 1, 2, and 3 was 2.11 mm/μsec. The average velocity based on peak strain was 1.39 mm/μsec. The theoretical shear velocity for the angle-ply was computed to be 1.58 mm/μsec. The agreement between the theoretical and experimental shear velocities is not as good as that in the in-plane velocity, c_0. The shape and magnitude of the pulses, however, do show fairly good agreement.

Figure 16 presents the comparison of the 25.4 mm striker induced strain histories on the angle-ply laminate with analysis. For this case, equation (9) predicted separation after $t = 4\ell/c_0$. Again, we note the general agreement of the pulse shapes and magnitudes. The average velocity based on first disturbance was 2.00 mm/μsec and based on peak strain was 1.78 mm/μsec. The theoretical shear velocity for the angle-ply was 1.58 mm/μsec.

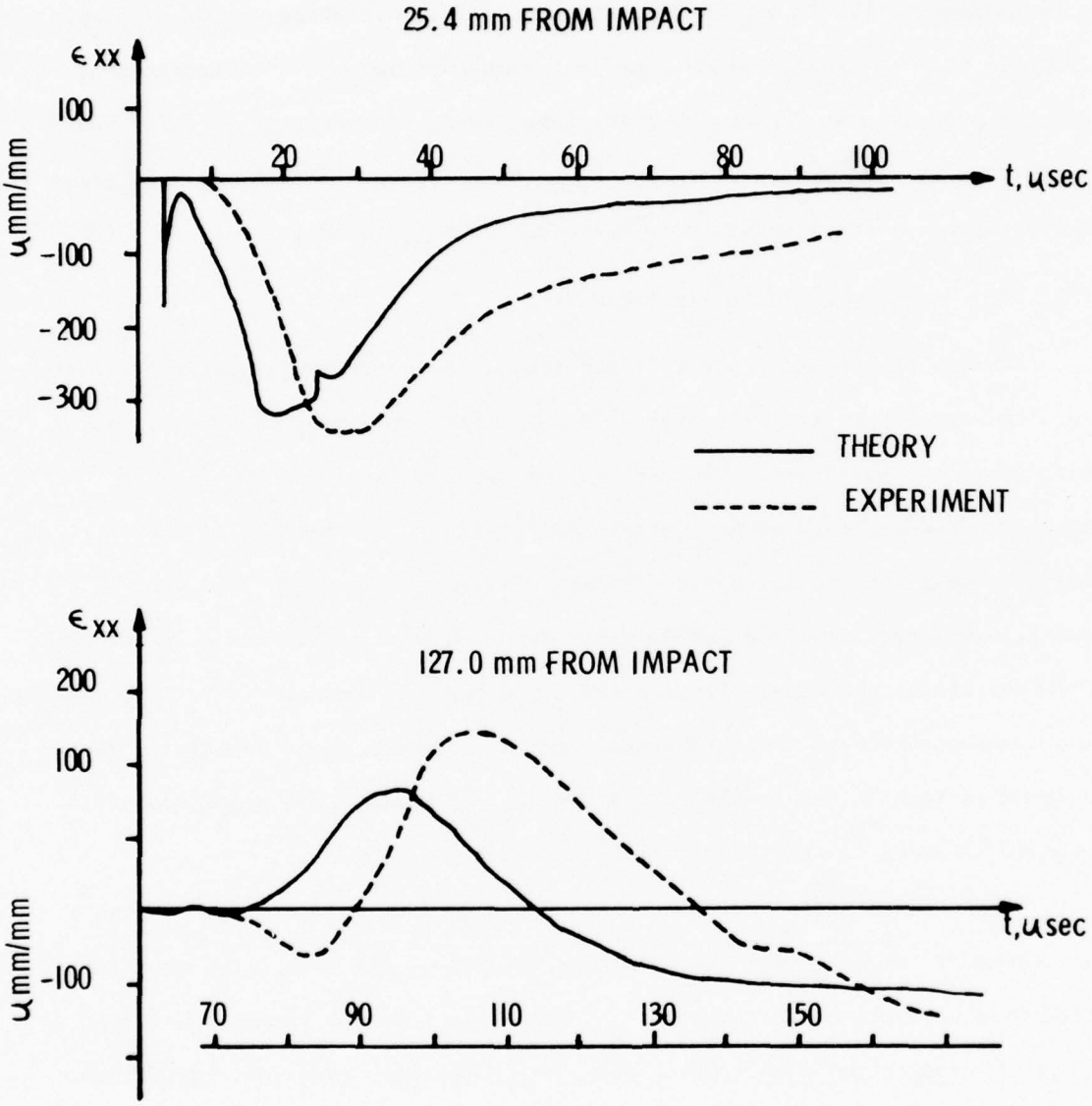

Figure 15. Theoretical and Experimental Strain Response of Angle-Ply Laminate Due to Transverse (Shear-Bending) Impact (76.2 mm Striker).

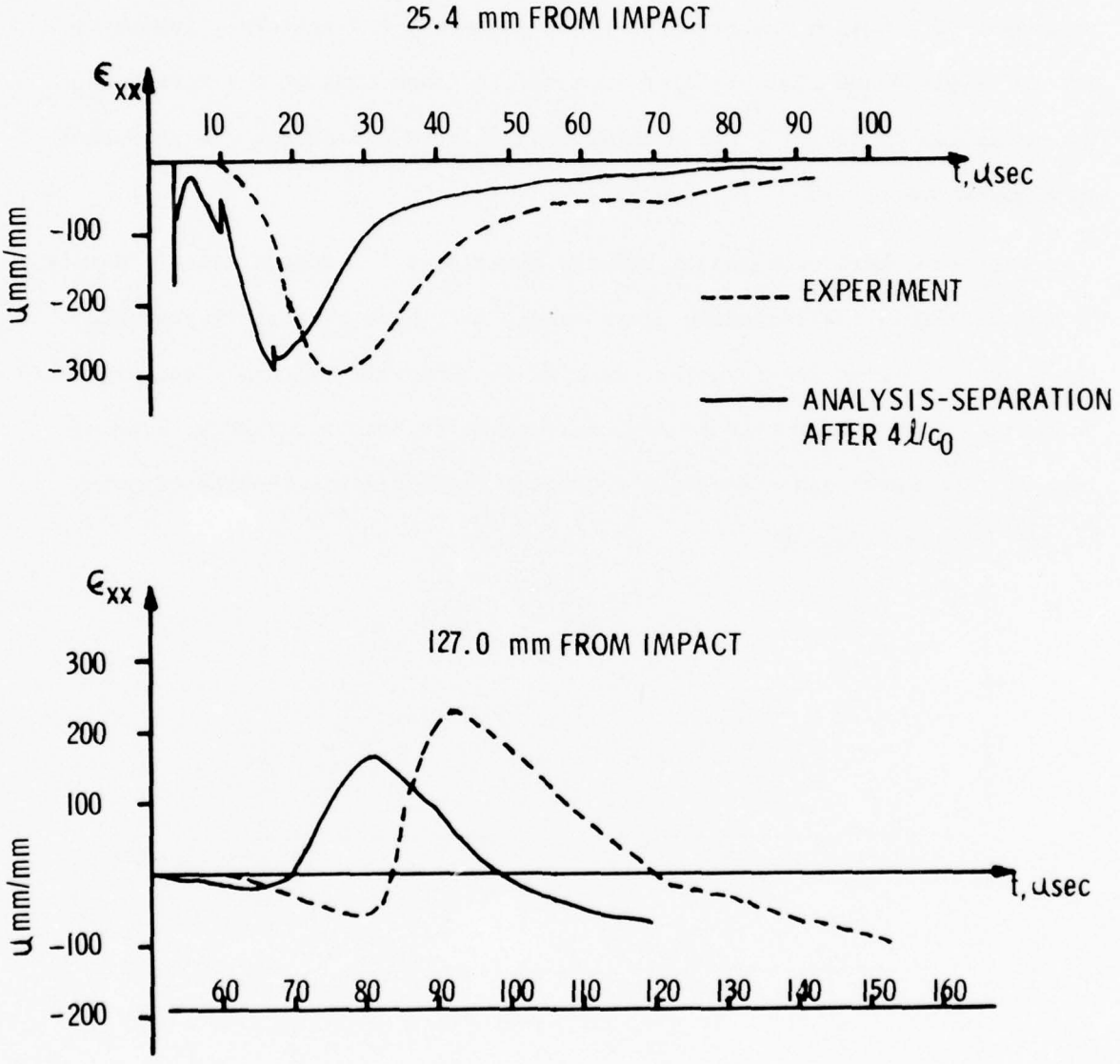

Figure 16. Theoretical and Experimental Strain Response of Angle-Ply Laminate Due to Transverse (Shear-Bending) Impact (25.4 mm Striker)

3. Summary and Conclusions

We have obtained, both experimentally and analytically, the transient responses of aluminum and graphite-epoxy cross-ply and angle-ply laminates due to in-plane and shear-bending impacts. A comparison of the wave speeds is summarized in Table 2 and a comparison of strain histories is presented in Figures 3,4,7,8,13,14,15, and 16.

Based on these comparisons between experimental and theoretical results, we conclude that the laminated plate theory used here adequately predicts the wave velocities and transient strains in symmetric cross-ply and angle-ply composite plates under either in-plane impact, or transverse shear-bending impact. The wave length to plate thickness ratio for the results reported here is approximately 8.

TABLE 2. SUMMARY OF WAVE SPEEDS

IMPACT CONDITION	SPECIMEN MATERIAL	STRIKER LENGTH (mm)	WAVE SPEEDS				
			IN-PLANE (mm/μsec)		SHEAR (mm/μsec)		
			EXP. (INT.)	THEORY	EXP. (PEAK)	EXP. (INT.)	THEORY
IN-PLANE	CROSS-PLY GRAPHITE-EPOXY	76.2	7.71	7.55			
		25.4	7.70	7.55			
	ANGLE-PLY GRAPHITE-EPOXY	76.2	7.54	7.39			
		25.4	7.32	7.39			
SHEAR-BENDING	CROSS-PLY GRAPHITE-EPOXY	76.2			1.67	1.81	1.53
		25.4			1.58	1.90	1.53
	ANGLE-PLY GRAPHITE-EPOXY	76.2			1.39	2.11	1.58
		25.4			1.78	2.00	1.58

III. STATUS OF LOCAL AND STRUCTURAL RESPONSE CALCULATIONS

1. HEMP - Local Response

We have made progress in modifying HEMP to accommodate anisotropic materials. We have incorporated into the code constitutive equations for general triclinic material in plane strain problems, and for transversely isotropic material for axisymmetrical problems. With slight further modification, the case of plane stress can be handled. We are in the process of debugging these modifications by running a sample problem. The following is a summary of the equations used in the anisotropic constitutive relations.

In as much as HEMP traces the position of the particle, it can be considered a Lagrangian program. However, the governing equations such as the equation of motion, constitutive relations, etc. are written with respect to coordinate system fixed in space. In this sense, HEMP could be considered as a hybrid Eulerian-Lagrangian computer code.

A composite can be "smeared" and treated as a homogeneous anisotropic material. The constitutive relation of HEMP has been modified to handle such cases in the elastic range. The new constitutive relations are

$$\dot{S}_{ij} = \frac{1}{3}\left[\, 3\, c_{ijk\ell} - c_{qqk\ell}\, \delta_{ij} \right] \dot{e}_{k\ell} + \frac{1}{3}\left[\, 3\, c_{ijkk} - c_{qqkk}\, \delta_{ij} \right] \dot{\varepsilon}_m + \dot{f}_{ij} \tag{10}$$

$$\dot{\sigma}_m = \frac{1}{3}\left[c_{iik\ell}\, \dot{e}_{k\ell} + c_{iikk}\, \dot{\varepsilon}_m \right] \tag{11}$$

where S_{ij} are the components of the deviator of the stress tensor; $e_{k\ell}$ are the components of the deviator of the strain tensor; σ_m is the spherical component of stress; ε_m is the mean normal strain; and $c_{ijk\ell}$ are the stiffness

constants relating stress and strain. The term f_{ij} is for transforming the previous state of stress into the current configuration and is given by

$$f_{ij} = a_{im}\, a_{jn}\, S^{0}_{mn} - S^{0}_{ij} \tag{12}$$

where a_{im} are the direction cosines and the superscript "0" signifies the previous state. The dot indicates the total time derivative. All indices in equations 10-12 run over 1,2,3. The other governing equations of HEMP remain essentially unchanged.

Equations 10-12 have been programmed to handle axisymmetrical and plane strain problems. Some slight modifications to HEMP still have to be made in order to handle plane stress problems. The axisymmetrical problems are limited to transversely isotropic materials; whereas, the plane strain case can handle up to a triclinic material. However, the plane strain case may later be modified to handle only up to a monoclinic material in order to save computation time.

As a means of debugging, an isotropic problem consisting of an iron cylinder impacting another iron cylinder has been run. Early indications are that Drexel's version of HEMP containing the previously mentioned anisotropic elastic constitutive relations gives good results. The next step in the debugging process will be to run a problem of a rigid cylinder impacting a semi-infinite composite of [0, $\pm$ 45, + 90] lay up. This composite can be "smeared" to give a homogeneous transversely isotropic material. Then the problem can be solved by HEMP as an axisymmetrical case.

2. NASTRAN - Structural Response

Three structural impact problems are presently being calculated by NASTRAN. One involves the transverse impact of a rod on a beam, the second involves the transverse impact of an angle-ply laminated plate (similar to the problem discussed in Section II-2) and the other involves a late-stage equivalence study in structural impact utilizing a laminated beam. The progress of each is discussed in the following paragraphs.

a. Transverse Impact of Rod on Beam-NASTRAN Analysis

An important objective of Drexel's F.O.D. research program is to obtain the transient elastic response of impacted structures. Unfortunately, most realistic F.O.D. impact problems are difficult to analyze due to the complicated geometries and loadings involved. In addition, these problems are further complicated by the use of anisotropic materials and laminated construction. Traditional analyses which utilize partial differential equations, such as the theory of elasticity or beam, plate, and shell theories, are practically limited to simple geometries and boundary conditions. Numerical methods, especially the finite element method, seems to be the only recourse. In the following sections an application of this method to a two-body impact problem will be presented.

F.E.M. Computer Code and Impact Problem

To solve complicated impact problems using the finite element method a computer code which possesses the following characteristics is necessary: a large number of types of elements, anisotropic material capability, flexible boundary condition modeling techniques, and more than one transient solution techniques. We believe that the NASTRAN (Ref. 18) computer code possesses these characteristics.

In order to compare our NASTRAN analysis with existing analytical and experimental results, we solved the problem of the normal impact of a semi-infinite isotropic rod on an infinite isotropic beam (Ref. 19). In the remaining sections, the details of the NASTRAN modeling of this impact problem and a comparison with the results (experiment and analysis) will be presented.

NASTRAN Boundary Condition Modeling

Because the rod is governed by the simple wave equation, the interaction of the rod on the beams can be approximated by an appropriate boundary condition on the beam. In addition, the symmetry condition is used. At the bar-beam interface, the local deformation of the beam is neglected, only the beam mode of deflection is considered. The force at the impact end of the bar, which is assumed to be equal to the shear in the beam, can then be calculated as a product of the acoustic impedance, cross-section area, and the velocity $(V_0 + \delta_{,t})$. In terms of the coordinate system shown in Fig. 17, the boundary conditions of the beam are x = 0

$$2Q = - \rho c A_r (V_0 + \delta_{,t}) \tag{13}$$

and

$$\theta = 0. \tag{14}$$

In equation (13), Q is the shear force, δ is the deflection of the beam, and ρ, c, and A_r are respectively the density, wave speed, and cross sectional area of the rod.

Equations (13) and (14) can be recast into finite element form by considering the impact to occur at node 1 and by making the following substitutions. Replace $Q|_{x=0}$ by an external force acting on node 1 in the y-dir., $F2^{(1)}$; also replace δ by the translational degree of freedom in the y-dir. at node 1, $U2^{(1)}$; and replace $\theta|_{x=0}$ by the rotational degree of freedom about the z-axis at node 1, $U6^{(1)}$. The equivalent finite element form of equations (13) and (14) are then

$$2F2^{(1)} + \rho cA_r U2,_t^{(1)} = - \rho cA_r V_0 \tag{15}$$

and

$$U6^{(1)} = 0 \tag{16}$$

For most finite element computer codes a boundary condition of the form of equation (15) cannot be used, however through the use of NASTRAN's transfer function capability equation (15) can be recast into an acceptable form. In essence, Equation (15) is treated as the governing equation of a fictitious element, with $F2^{(1)}$ and $\rho cA_r V_0$ as the two displacements of the element. Due to the $U2,_t^{(1)}$ term, the viscous damping matrix must be used although it has only one non-zero term. This fictitious element adds two additional rows and columns to all matrices.

To accomplish this, we first augment the matrix governing equations by two rows and columns. This is accomplished by using an EPOINT bulk data card. Call these non-structural degrees of freedom e_{100} and e_{200}, and take e_{100} equal to $F2^{(1)}$ and e_{200} equal to $\rho cA_r V_0$. Second, from the finite element equation for $F2^{(1)}$ in terms of the discrete degrees of freedom obtain an equation which relates e_{100} to the appropriate discrete degrees of freedom. This equation has the following form

$$M2^{(1)}U2,_{tt}^{(1)} + M2^{(2)}U2,_{tt}^{(2)} + M6^{(2)}U6,_{tt}^{(2)} + K2^{(1)}U2^{(1)} + K2^{(2)}U2^{(2)} + K6^{(2)}U6^{(2)} - e_{100} = 0 \tag{17}$$

where the M's are the consistent mass terms and the K's are the stiffness terms. Third, use e_{100} and e_{200} to recast equation (15) into the following

$$2e_{100} + \rho cA_r U2,_t^{(1)} + e_{200} = 0. \tag{18}$$

Finally define an external loading on e_{200} such that

$$e_{200} = \rho cA_r V_0. \tag{19}$$

The result of this procedure is that $F2^{(1)}$ is defined implicitly as a function of $U2,_t^{(1)}$. Equations (17) and (18) are generated in NASTRAN by use of TF bulk data cards. Equation (19) is generated in two steps. First a TF bulk data card is used to generate the left hand side of the equation, and second TLOAD1,

TABLE1, and DAREA bulk data cards are used to generate the load $\rho c A_r V_0$. Note for quiescent initial conditions the value of $\rho c A_r V_0$ must be fast ramped. The preceding procedure was utilized to affect boundary condition (15) in our NASTRAN analysis.

NASTRAN Problem and Comparison with Experiment

The finite element geometry used in the analysis is shown in Fig. 17. The discretization was chosen in order that we could accurately include all modes up to the fifteenth symmetric mode, and the overall length of the beam was chosen so that the solution at x = 25.4 mm and 76.2 mm, would not be influenced by wave reflection from the boundary for at least 100 μsec.

The stiffness matrix was formed from beam elements which have a shear deflection correction and the mass matrix was formed by the consistent approach. The transient equations were solved using NASTRAN's direct integration, rigid format. The time step chosen at Δt = 0.5 μsec. which is approximately one third of the period of the fifteenth mode.

In Fig. 18 a comparison is presented between the NASTRAN solution and the analytical and experimental results of Ref. [19], for the normal impact of a rod and beam. The NASTRAN solution is in good agreement with the experimental results. The analytical solution of Ref. [19] was obtained from numerical inversion of the Laplace transformation of the Timoshenko beam equations with boundary conditions (13) and (14). The NASTRAN solution does pick up the change in shape of the response at x = 1" and x = 3", and it does reasonably yield the peak response at these two locations. Oscillations in the NASTRAN solution may be eliminated by using a smaller time step.

On the basis of the good agreement between the NASTRAN solution and the experimental data for this two body impact problem, we will apply this technique to more complicated two-body impact problems.

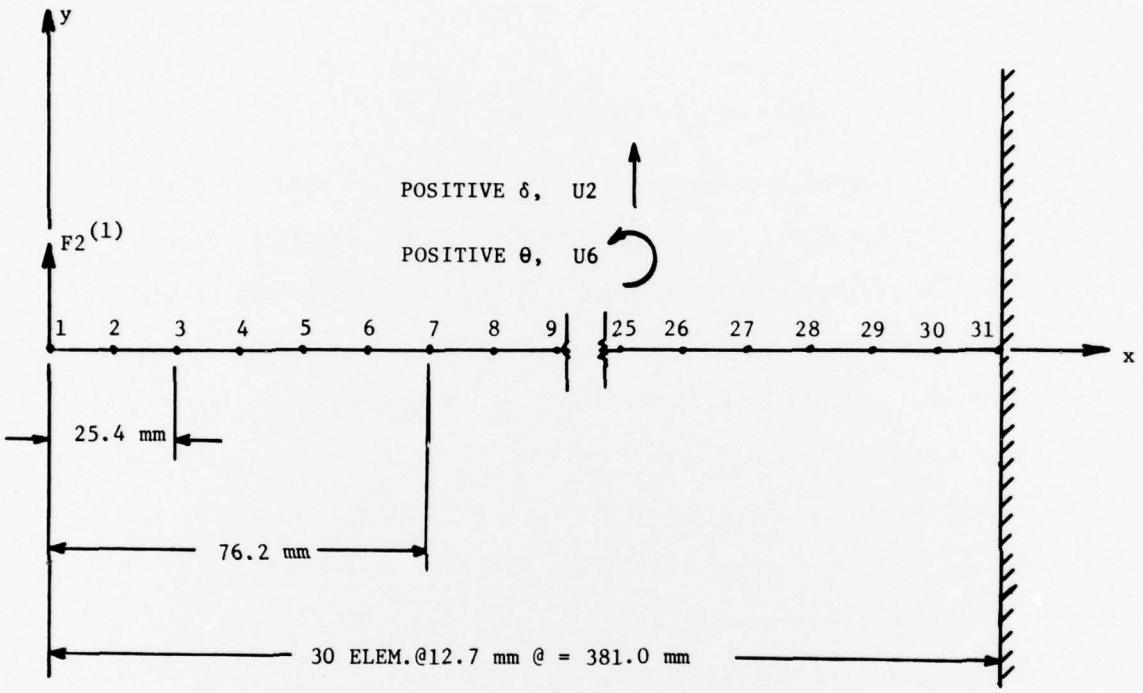

BOUNDARY CONDITIONS

NODE 1: $2F2^{(1)} + \rho\, cA_r\, U2_{,t}^{(1)} = -\rho\, cA_r\, V_0$

$U6^{(1)} = 0$ (SYMMETRY)

NODE 31: $U2^{(31)} = U6^{(31)} = 0$ (FIXED)

INITIAL CONDITIONS

t = 0: $U2^{(i)} = U6^{(i)} = 0 \qquad i = 1,2,\ldots,31$

$U2_{,t}^{(i)} = U6_{,t}^{(i)} = 0$

Figure 17. Finite Element Geometry and Auxiliary Conditions

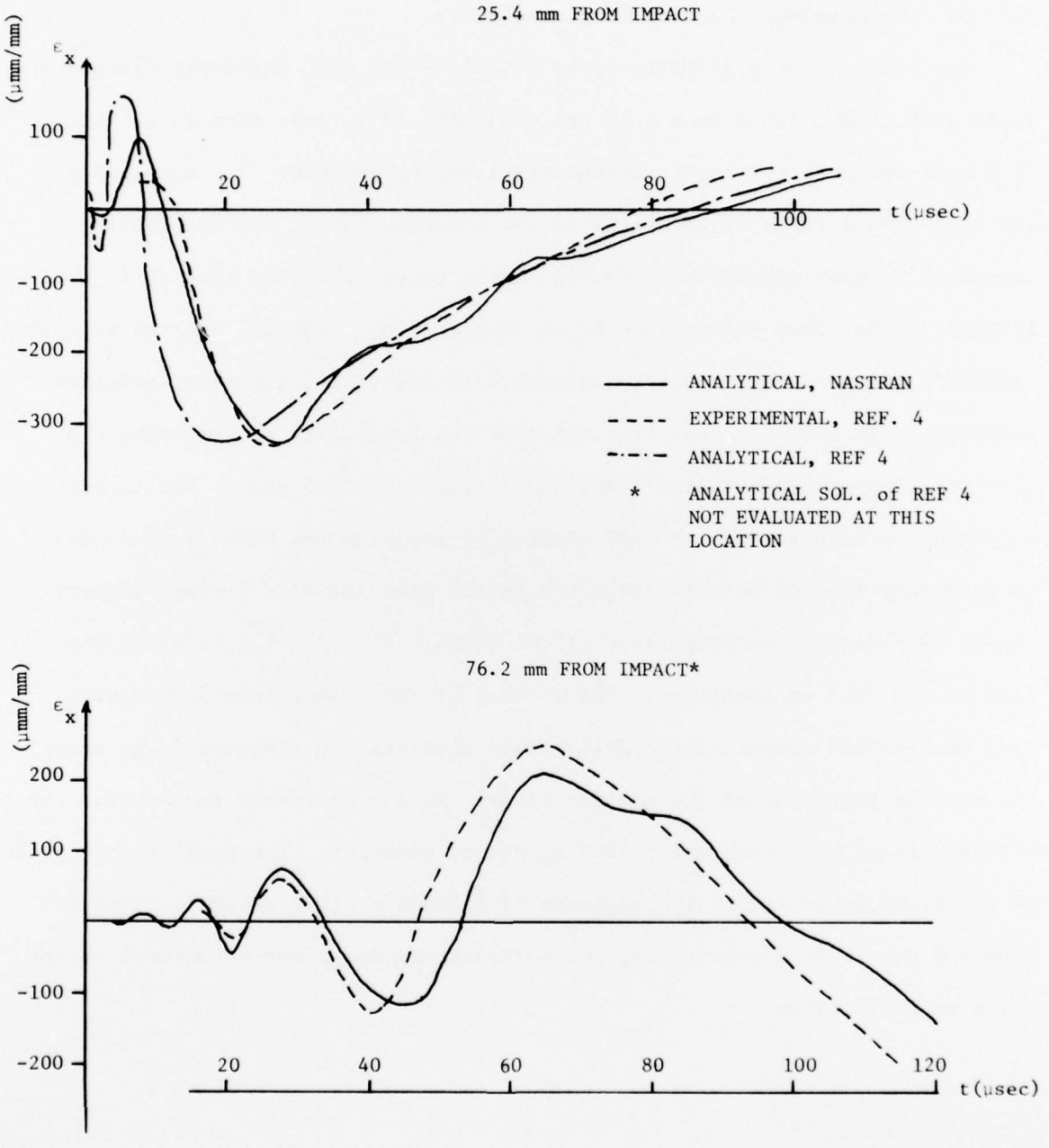

Figure 18. NASTRAN SOLUTION OF THE IMPACT OF A SEMI-INFINITE STEEL ROD ON AN INFINITE STEEL BEAM

b. Transverse Impact of Laminated Plate

The response of a graphite-epoxy $[(0/45/0/-45)_6/0]_S$ angle-ply laminated plate (609.6 mm x 355.6 mm x 7.11 mm) subjected to a transverse shear impact by a semi-infinite striker is being calculated by NASTRAN. The material and lay-up of the striker is identical to the impacted plate; the problem is identical to that described in Section II-2e except that the striker is semi-infinite rather than either 25.4 mm or 76.2 mm long. Our initial run utilized NASTRAN's plate element (25.4 mm square) with the direct transient solution technique. We have used the transfer function capability to prescribe the two-body impact boundary conditions and a time step of 5 μsec. For comparison purposes, we have solved the same problem by applying the MCDU-22 code [20] to equations (3c) of Ref. 14 subjected to the semi-infinite striker impact. Figure 19 presents the comparison of the transient strain histories at the 25.4 mm and 76.2 mm locations. The results of this comparison demonstrate that the NASTRAN computation qualitatively predicts the response (e.g. shape) but not the magnitude at the earlier times. We are presently recomputing the NASTRAN strain histories using 12.7 mm square elements. The goal of this phase of the study is to assess the adequacy of NASTRAN's plate elements, impact boundary condition prescription, and solution technique for structural impact response predictions.

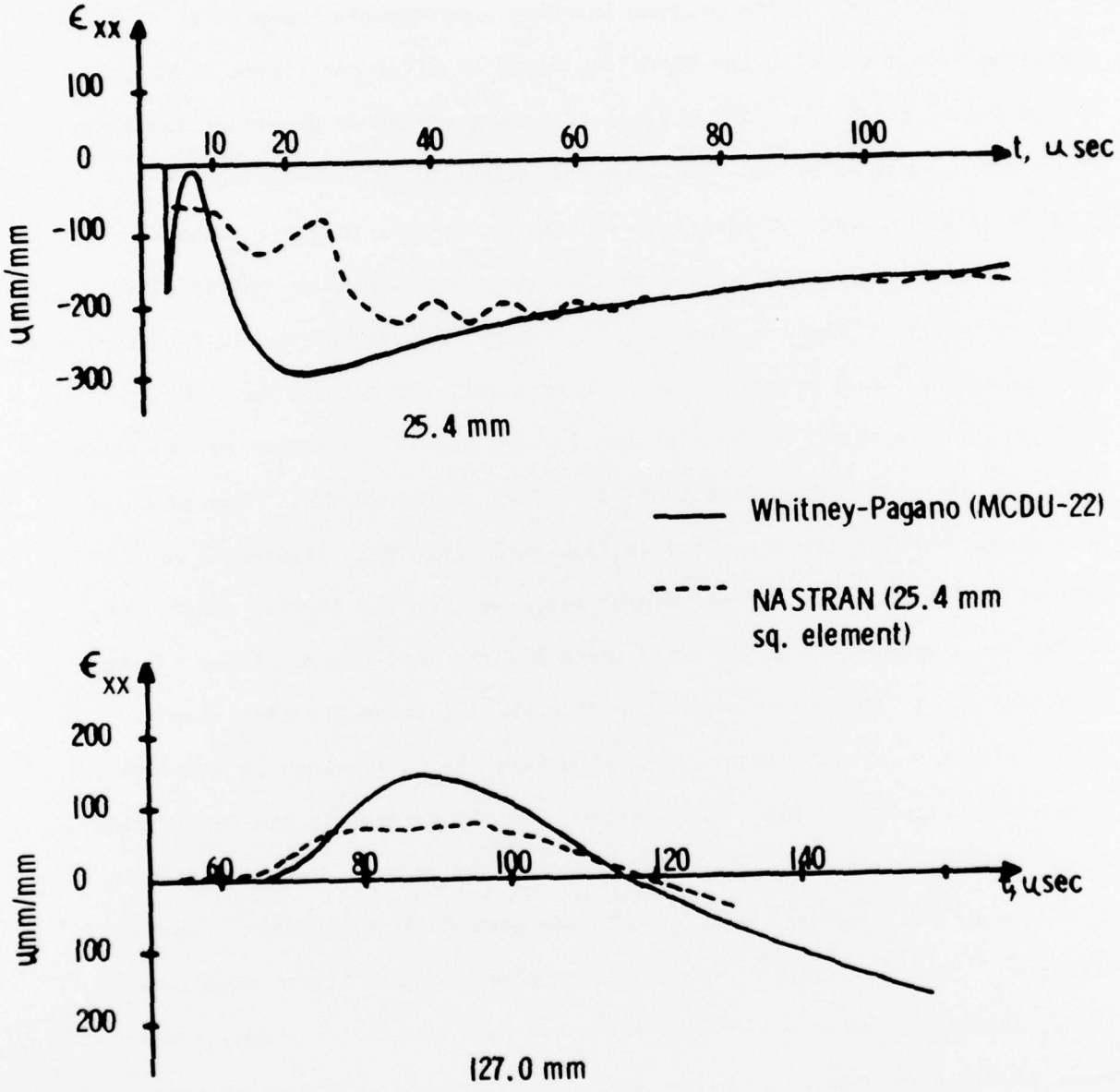

Figure 19. NASTRAN Solution of Transient Response of Angle-Ply Laminate to Transverse Shear-Bending Impact

c. Late-Stage Equivalence Study in Structural Impact

This phase of the program involves a parametric study of a laminated beam model of a fan blade subjected to different impact loadings on the end of the blade. The purpose of this study is to determine the late-stage equivalence of structural responses caused by impacts defined by similar or dissimilar parameters (e.g. kinetic energy, impulse, pulse shape, and pulse duration). Figure 20 describes the overall problem and NASTRAN modelling being utilized in this study. Figure 21 describes the loading impact parameters used for each part of this study. To date we have obtained 1000 μsec of transient response at the 5", 10" and 19" locations of the blade model for each of loading conditions described in Figure 21 . Some of these preliminary results are presented in Figures 22 thru 25. Figures 22 and 23 present the transient shear and moment responses for the loading conditions having equal impulses. We see from these Figures that the magnitude of the responses due to the larger magnitude (but smaller pulse duration) input pulse is initially much larger, but, with time this difference in response magnitudes decreases. This trend is particularly evident at the 19" location. Figures 24 and 25 present the transient shear and moment responses for the loading conditions having equal kinetic energies (elastic striker - unequal impulses). For this case we see that the pulse with the higher magnitude (lower impulse) produces responses which are much smaller at longer times. These preliminary results indicate that the impulse is an important parameter in any impact boundary condition specification. We are presently computing some of the responses for 1500 μsec to verify the aforementioned trends and are plotting the results for the pulse duration and pulse shape studies.

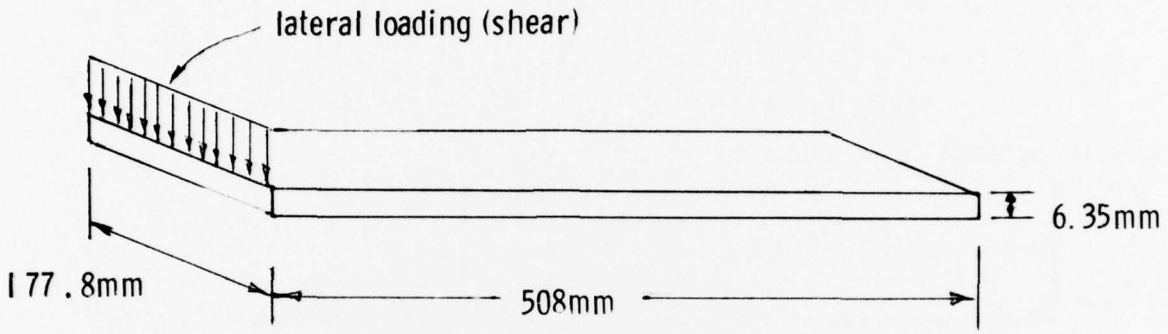

- MATERIAL = GRAPHITE EPOXY
- LAY-UP = $\left[(0/\pm 22)_8/0\right]_S$
- ELEMENTS = 40 BEAM ELEMENTS
- LOADING = SHEAR
- LOADING IMPACT PARAMETERS
  - IMPULSE
  - KINETIC ENERGY
  - SHAPE
  - PULSE DURATION
- SOLUTION = MODAL TRANSIENT (NASTRAN)
  - 20 MODES

Figure 20. Late-Stage Equivalence in Structural Impact-Problem Description

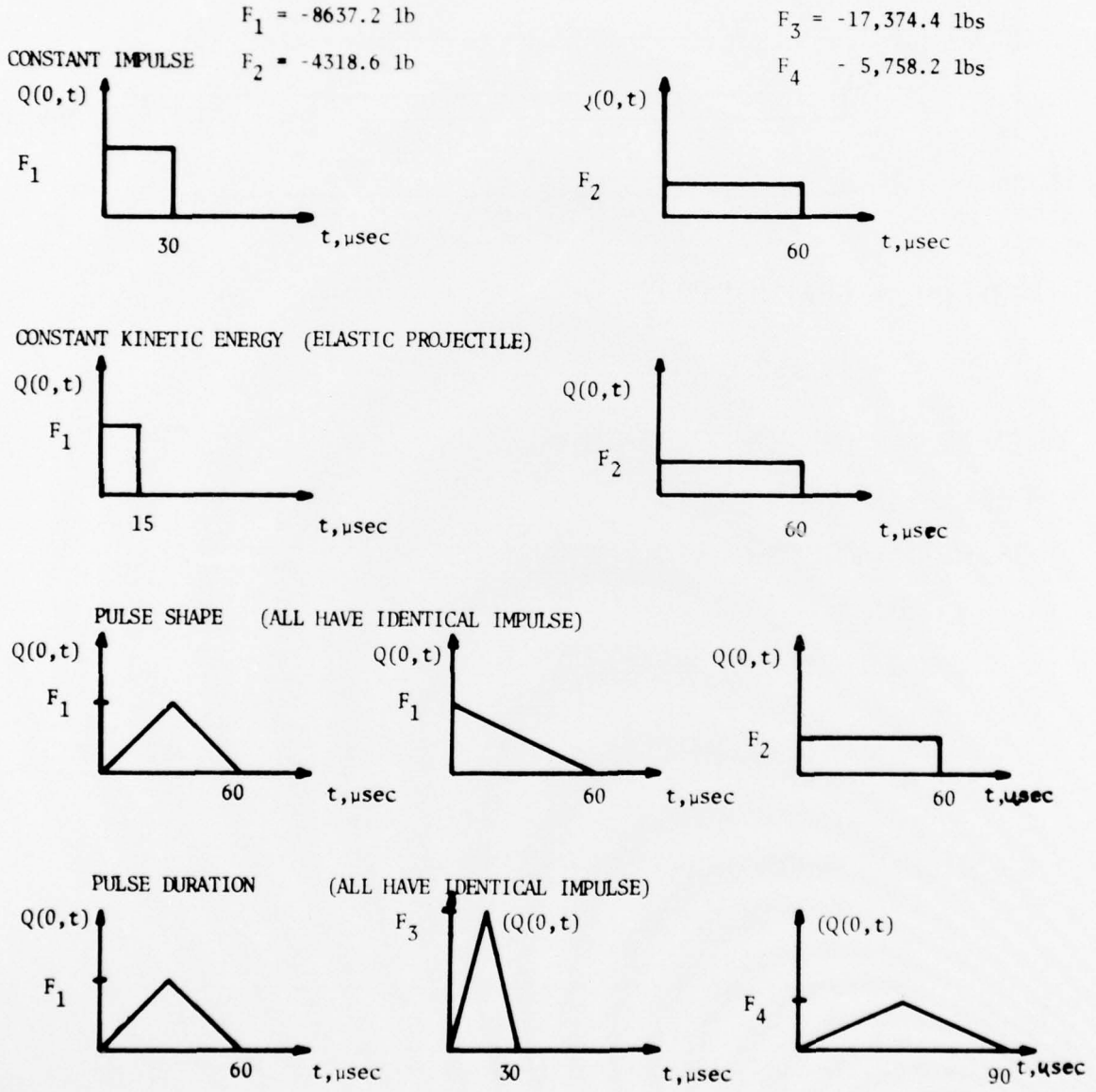

Figure 21. Load Impact Parameters Used in Late-Stage Equivalence Study

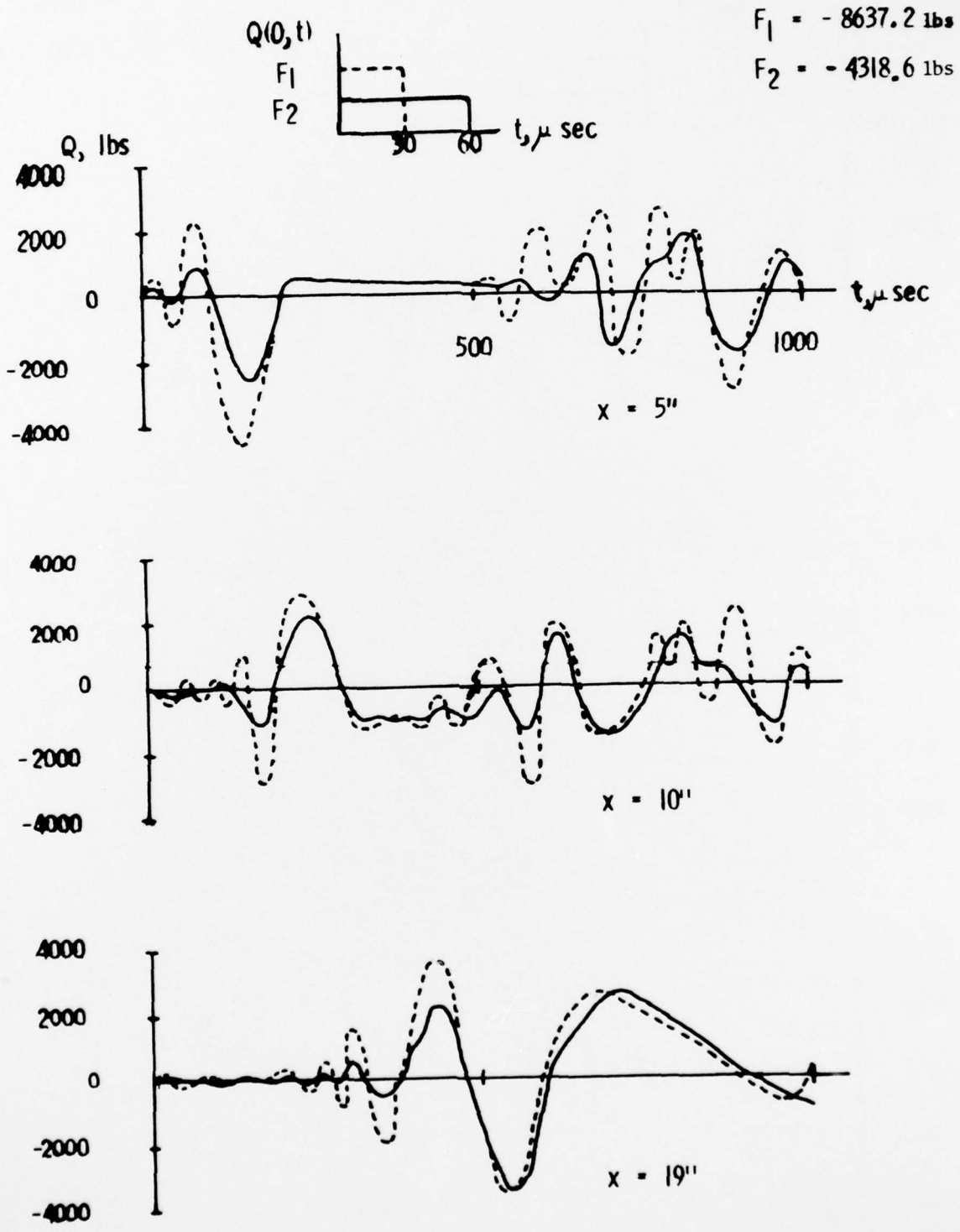

Figure 22. Transient Shear Response for Loading Conditions Having Equal Impulses

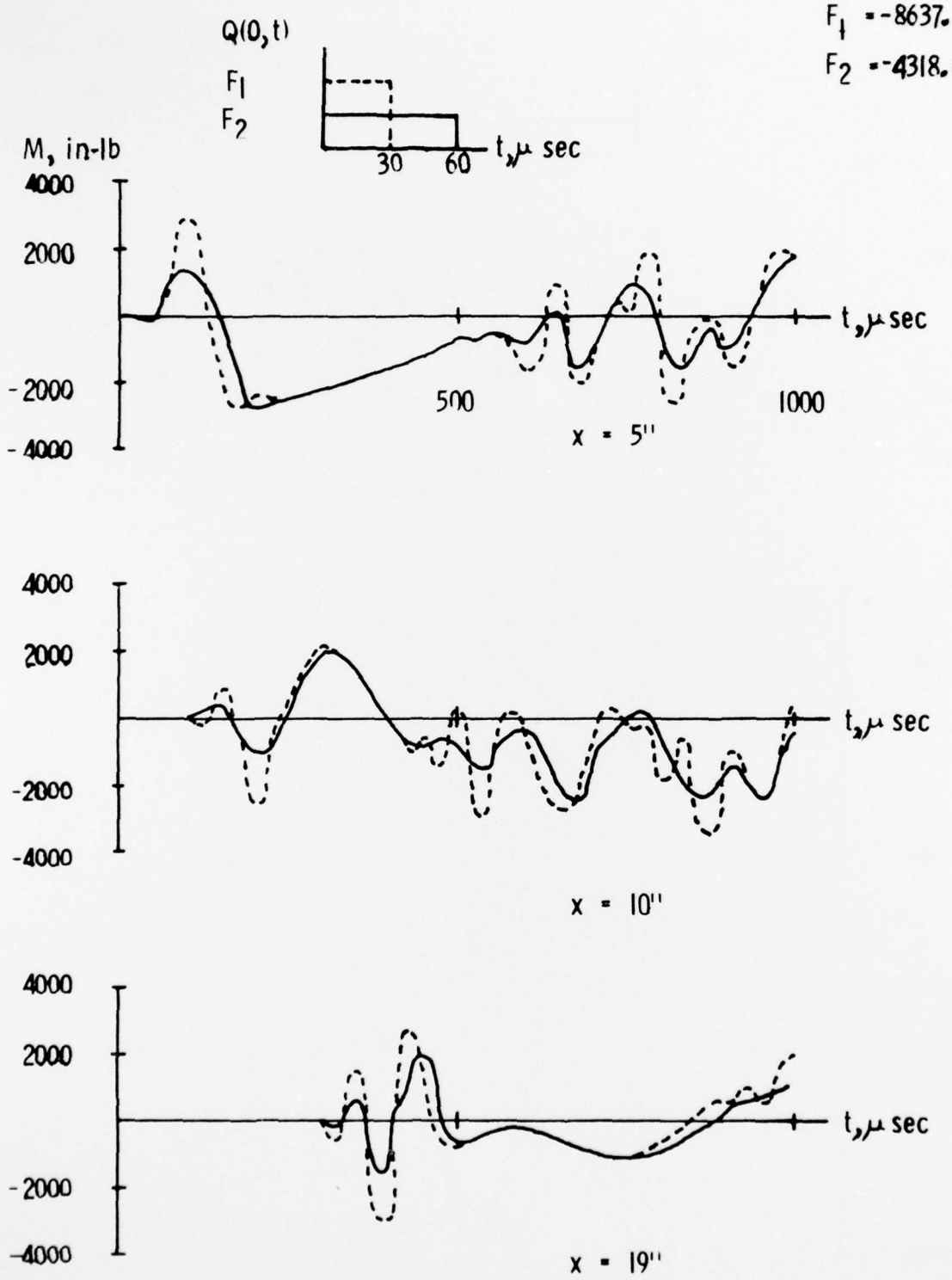

Figure 23. Transient Moment Response for Loading Conditions Having Equal Impulse

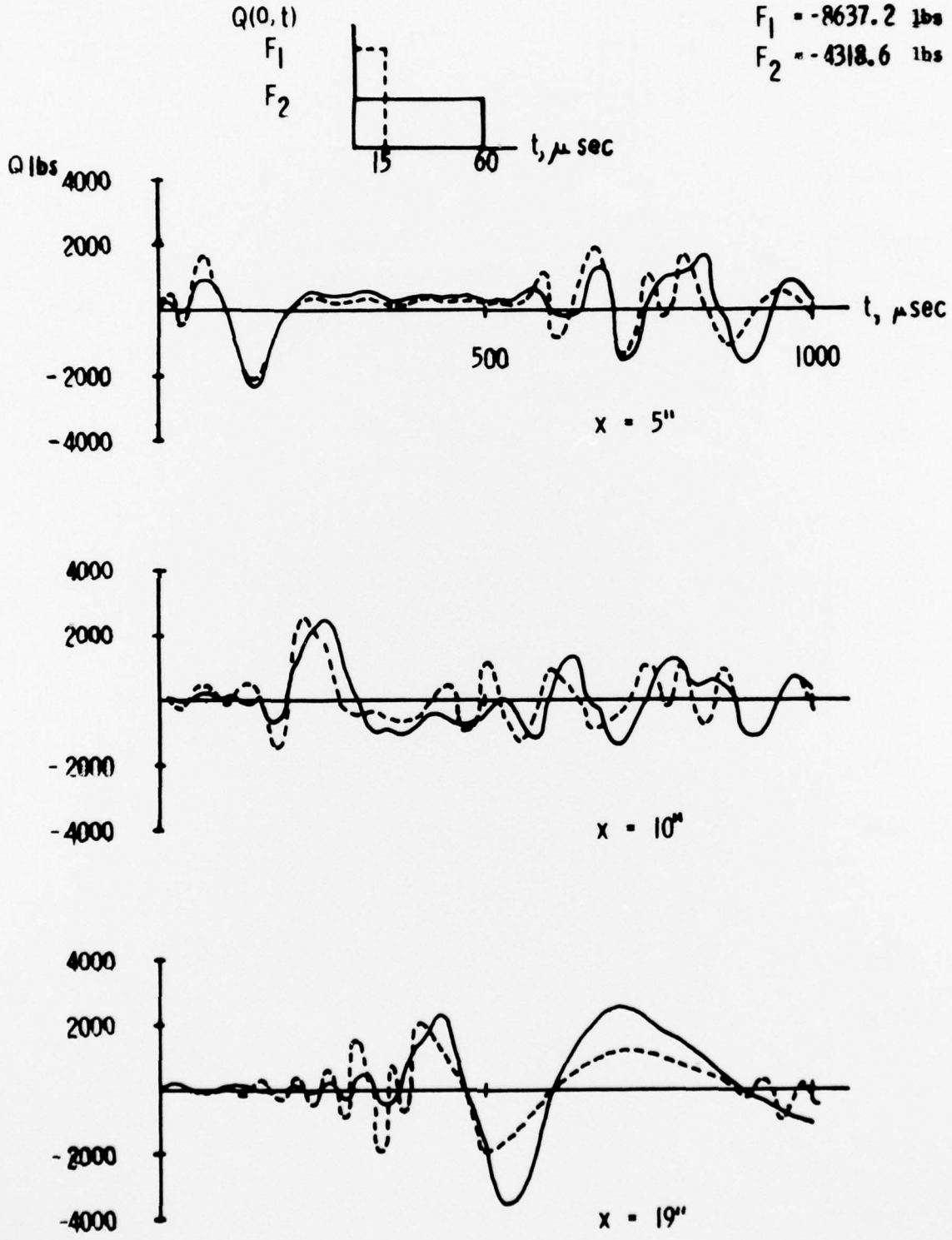

Figure 24. Transient Shear Response for Loading Conditions Having Unequal Impulses

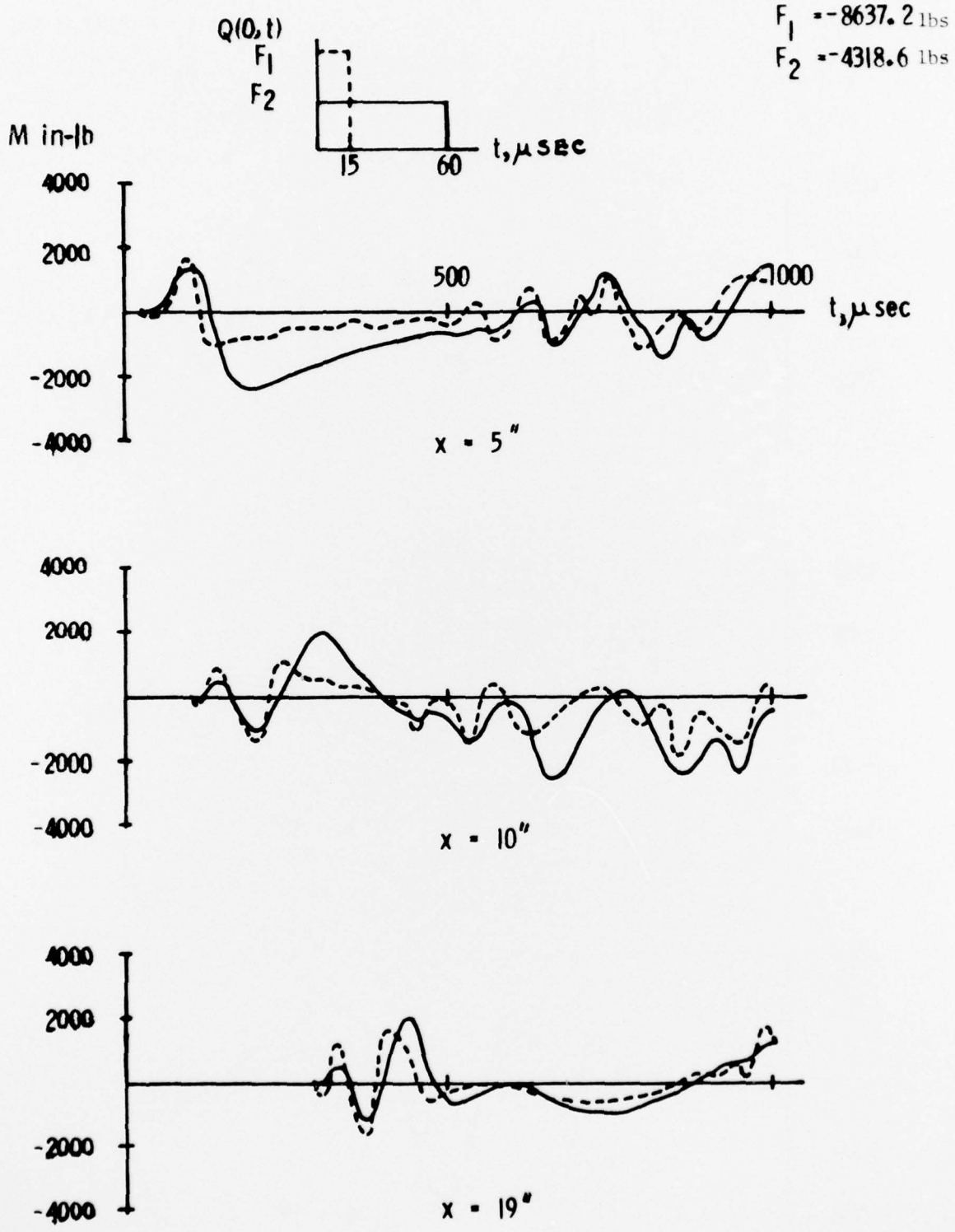

Figure 25. Transient Moment Response for Loading Conditions Having Unequal Impulses.

REFERENCES

1. Stuber, C.C., "Minutes of AFML FOD Meeting", AFML/LL, Wright-Patterson Air Force Base, Ohio, May 1972.

2. Whitney, J.M. and Pagano, N.J., "Shear Deformation in Heterogeneous Anisotropic Plates," J. Aerospace Sci., Vol. 29, No. 8, pp. 969-975, 1962.

3. Wang, A., and Chou, P., "A Comparison of Two Laminated Plate Theories," Jour. Appl. Mechs, pp. 611-613, June 1972.

4. Yang, P., Norris, C., and Stavsky, Y., "Elastic Wave Poopagation in Heterogeneous Plates," Int. Jour. Solids and Structures, Vol. 2, pp. 665-684, 1966.

5. Wang, A. and Tuckmantel, D., "Elastic Wave Surfaces in Heterogeneous Anisotropic Plates," AIAA Jour. Vol. 11, No. 11, pp. 1571-1573, Nov. 1973.

6. Moon, F.C., "Wave Surfaces Due to Impact on Anisotropic Plates," J. Comp. Mat., Vol. 6, pp. 62-79, 1972.

7. Chow, T.S., "On the Propagation of Flexural Waves in an Orthotropic Laminated Plate and Its Response to an Impulsive Load," J. Comp. Mat., Vol. 5, pp. 306-319, July 1971.

8. Moon F.C., "One Dimensional Transient Waves in Anisotropic Plates," J. Appl. Mech., pp. 485-490, June 1973.

9. Sun, C.T. and Lai, R.Y., "Exact and Approximate Analysis of Transient Wave Propagation in An Anisotropic Plate," AIAA Journal, pp. 1415-1417, Oct. 1974.

10. Whittier, J.S. and Peck, J.C., "Experiments on Dispersive Pulse Propagation in Laminated Composites and Comparison with Theory," J. Appl. Mech., Vol. 36, pp. 485-490, Sept. 1969.

11. Tauchert, T.R. and Guzelsu, A.N., "An Experimental Study of Dispersion of Stress Waves in a Fiber-Reinforced Composite," J. Appl. Mech., Vol. 39, pp. 98-102, March 1972.

12. Tauchert, T.R. and Moon, F.C., "Propagation of Stress Waves in Fiber-Reinforced Composite Rods," AIAA/ASME 11th Structures, Structural Dynamics and Materials Conference, Denver, Colorado, 1970.